# Aqueous behaviour of characteristic molecules in the synthesis of porous silica materials

## - an atomistic description

Nilsson, Emelie

2016

# Aqueous behaviour of characteristic molecules in the synthesis of porous silica materials

## – an atomistic description

PHYSICAL CHEMISTRY | LUND UNIVERSITY
EMELIE J. NILSSON

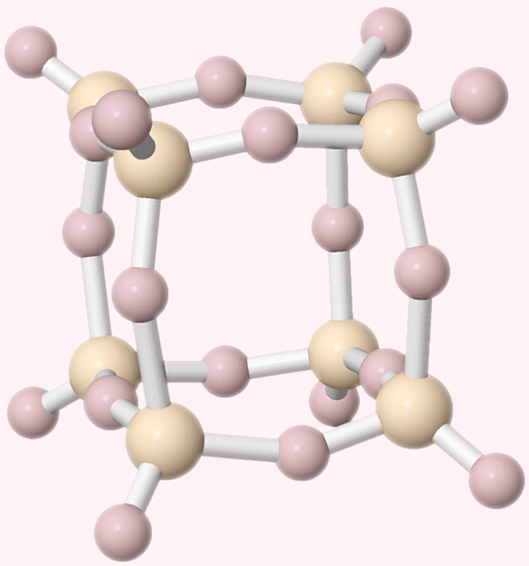

# Aqueous behaviour of characteristic molecules in the synthesis of porous silica materials

## - an atomistic description

**Emelie J. Nilsson**

LUND
UNIVERSITY

DOCTORAL DISSERTATION
by due permission of the Faculty of Science, Lund University, Sweden.
To be defended on 13 June 2016, at 10.00 in lecture hall B, Centre for Chemistry and Chemical Engineering, Lund

*Faculty opponent*

Professor Ferdi Schüth, Max-Planck-Institut für Kohlenforschung, Mülheim, Germany

Organization
**LUND UNIVERSITY**

Division of Physical Chemistry
Box 124
221 00 LUND
Sweden

Author(s)
Emelie J. Nilsson

Document name
DOCTORAL DISSERTATION

Date of issue
2016-05-17

Sponsoring organization
Swedish research council

Title and subtitle
Aqueous behaviour of molecules characteristic in the the synthesis of porous silica material – an atomistic description.

Abstract
The formation process of porous silica materials is an intricate process, involving a number of components that interact to form a highly organized material. Both zeolites and mesoporous silica materials typically require the presence of organic structure director agents (SDAs) around which the silica network polymerizes. For zeolites the SDAs are molecular and for mesoporous silica the SDAs assemble into aggregates, i.e. micelles. The aim of this thesis is to further the understanding of the initial stages of the formation of porous silica materials. This has been done by investigating aqueous model systems of components critical for the formation of porous silica materials using neutron scattering coupled with empirical potential structure refinement (EPSR) to arrive at atomistic descriptions of the systems. The systems are based on aqueous solutions of single components under different conditions as well as a system in which two components are mixed and allowed to interact. Molecular SDAs, tetramethylammonium bromide and tetrapropylammonium bromide respectively, were found to have different association behavior; small clusters of tetrapropylammonium ions were formed whereas tetramethylammonium only formed pairs. Micellar SDA aggregates of decyltrimethylammonium ions with different counterions reveal a strong dependence on the identity of the counterions. The effect of the counterions appears to originate from a subtle balance between electrostatic interactions and ion-specific effects. A model system for oligomeric silica species was evaluated. The system is based on cubic silsesquioxane. $^{29}$Si NMR was used to identify and quantify the silica species that occur in solution. The silica species reveal a high dependence on additives in solution, which can stabilise the cubic silica molecule. Finally the silica model was probed in the presence of decyltrimethylammonium ions in order to probe interactions that occur in the early stages of the synthesis of MCM-41. The silica species show little affinity for the micelle surface, even though being negatively charged, however their presence in the system greatly decrease the size of the micelles compared to those in a pure aqueous solution.

Key words
Porous silica, struture directing agents, 29Si-NMR, neutron scattering, empirical potentail structure refinement, micelles

Classification system and/or index terms (if any)

Supplementary bibliographical information

Language

ISSN and key title

ISBN
978-91-7422-452-8

Recipient´s notes

Number of pages
146

Price

Security classification

Distribution by (name and address)



Signature  Date 2016-05-02

# Aqueous behaviour of characteristic molecules in the synthesis of porous silica materials

## - an atomistic description

**Emelie J. Nilsson**


LUND
UNIVERSITY

Cover: illustration of the cubic silicate species, depicted with a ball and stick representation.

Division of Physical Chemistry | Department of Chemistry | Lund University

ISBN 978-91-7422-452-8 (print)
ISBN 978-91-7422-453-5 (electronic)

Printed in Sweden by Media-Tryck, Lund University
Lund 2016

# Contents

# List of Papers

This thesis is based on the following papers, which will be referred to in the text by their Roman numerals. The papers are appended at the end of the thesis.

I **A neutron scattering and modelling study of aqueous solutions of tetramethylammonium and tetrapropylammonium bromide**
Emelie J. Nilsson, Viveka Alfredsson, Daniel T. Bowron and Karen J. Edler
*Physical Chemistry Chemical Physics*, 2016, **18**, 11193 - 11201

II **Effect and arrangment of counterions on decyltrimethylammonium surfactants**
Emelie J. Nilsson, Daniel T. Bowron, Olle Söderman, Viveka Alfredsson and Karen J. Edler
*Manuscript*

III **Stability and behaviour of the cubic silsesquioxane, $Si_8O_{20}^{8-}$, in aqueous solutions**
Emelie J. Nilsson, Marina Huber, Göran Carlström, Olle Söderman, Daniel T. Bowron, Karen J. Edler and Viveka Alfredsson
*Manuscript*

IV **Interactions between cationic micelles and small silica oligomers**
Emelie J. Nilsson, Daniel T. Bowron, Karen J. Edler and Viveka Alfredsson
*Manuscript*

## List of Contributions to the papers

I EJN analysed the data and was main responsible for writing the paper.

II EJN participated in the design of the project. EJN performed all the experiments with help from DTB, VA and KJE, analysed the data and was main responsible for writing the paper.

III EJN participated in the design of the project. EJN performed the scattering experiments with help from DTB, VA and KJE, was responsible for the design and measurement of the Si-NMR, analysed the data and was main responsible for writing the paper.

IV EJN participated in the design of the project. EJN performed the scattering experiments with help from DTB, VA and KJE, was responsible for the Si-NMR measurements, analysed the data and was main responsible for writing the paper.

# Abstract

The formation process of porous silica materials is an intricate process, involving a number of components that interact to form a highly organized material. Both zeolites and mesoporous silica materials typically require the presence of organic structure director agents (SDAs) around which the silica network polymerizes. For zeolites the SDAs are molecular and for mesoporous silica the SDAs assemble into aggregates, i.e. micelles. The aim of this thesis is to further the understanding of the initial stages of the formation of porous silica materials. This has been done by investigating aqueous model systems of components critical for the formation of porous silica materials using neutron scattering coupled with empirical potential structure refinement (EPSR) to arrive at atomistic descriptions of the systems. The systems are based on aqueous solutions of single components under different conditions as well as a system in which two components are mixed and allowed to interact. Molecular SDAs, tetramethylammonium bromide and tetrapropylammonium bromide respectively, were found to have different association behavior; small clusters of tetrapropylammonium ions were formed whereas tetramethylammonium only formed pairs. Micellar SDA aggregates of decyltrimethylammonium ions with different counterions reveal a strong dependence on the identity of the counterions. The effect of the counterions appears to originate from a subtle balance between electrostatic interactions and ion-specific effects.

A model system for oligomeric silica species was evaluated. The system is based on cubic silsesquioxane. $^{29}$Si-NMR was used to identify and quantify the silica species that occur in solution. The silica species reveal a high dependence on additives in solution, which can stabilise the cubic silica molecule. Finally the silica model was probed in the presence of decyltrimethylammonium ions in order to probe interactions that occur in the early stages of the synthesis of MCM-41. The silica species

show little affinity for the micelle surface, even though being negatively charged, however their presence in the system greatly decrease the size of the micelles compared to those in a pure aqueous solution.

# Abbreviations

| | |
|---|---|
| $C_{10}TA^+$ | decyltrimethylammonium |
| CMC | critical micelle concentration |
| EPSR | empirical potential structure refinement |
| EP | Empirical Potential |
| MCM-41 | Mobil Composition of Matter 41 |
| NMR | Nuclear magnetic resonance |
| SDA | structure directing agent |
| $TMA^+$ | tetramethylammonium ion |
| $TPA^+$ | tetrapropylammonium ion |

# Symbols and Constants

| | |
|---|---|
| $a_0$ | effective headgroup area |
| $\beta$ | Counterion dissociation |
| $\epsilon_0$ | permittivity in vacuum |
| $\varepsilon_{\alpha\beta}$ | the depth parameter in a Lennard-Jones potential |
| $\kappa$ | specific conductivity |
| $k$ | Boltzmann's constant |
| $N_{agg}$ | micelle aggregation number |
| $N_s$ | surfactant packing parameter |
| $R$ | Resistivity |
| $R$ | radius of gyration |
| $\sigma_{\alpha\beta}$ | the range parameter in a Lennard-Jones potential |
| $T$ | temperature |

# Chapter 1

# Introduction

Porous materials have been of interest for a long time due to their extensive use and it is desirable to find ways to tune the properties of these materials. Two fundamental properties of porous materials are the size and structure of the pores. The pores can have random orientations, as in a bath sponge, or be organized, as in for instance a honeycomb. The applications put demands on the properties that the material must have to function optimally. For instance a drug carrier, would benefit from a pore structure that controls the release rate together with a pore size that allows the drug molecules to be freely loaded into the material, while an absorbent would benefit from having a large pore volume.

Silica, silicon dioxide ($SiO_2$), is present, or the main component, in many materials, e.g. zeolites, glass, quarts, insulators in electronics, ceramics and diatoms. Silica can be found both in an amorphous form (e.g. glass) or in a crystalline state (e.g. quarts). Porous silica materials can have a vast range of pore sizes and structures and can be found in both crystalline and amorphous states. Due to the materials' overall characteristics and multitude of uses, they have been receiving a lot of attention. Studies have been devoted to find ways to alter the materials to fit the ever changing needs of new appplications. However the formation process of these materials are yet to be completely characterised. A full understanding of the formation process would allow for rational design of the materials.

The porous material typically form in an process where an important component is a structure directing agent. The structure directing agent

can function on its own or in supramolecular aggregates, i.e. in a micelle. The pores in the material are opened as the structure directing agent is removed. Present in the formation process is also a silica source, which at the optimum conditions polymerize and forms the material around a structure director. The porous silica materials are formed during a co-operative process of condensating silica and the rearrangement of the structure directors.

The aim of this work is to forward the understanding of the formation process of porous silica materials, with a focus on the structure directing agents. Both structure directing agents for zeolite synthesis, i.e. tetramethylammonium ions and tetrapropylammonium ions, and for mesoporous silica materials, i.e. decyltrimethylammonium, have been studied.

We have devised model systems aimed at examining the molecular behaviour at the very initial stages of the formation process. The model systems are designed to to probe different components as well as more complex systems. The structure directing agents, for zeolites and mesoporous materials, were investigated in the first two papers. In the third paper an evaluation of the the molecular silica model is performed. In the fourth paper, the molecular silica model is combined with the structure directing agent for mesoporous silica, the decyltrimethylammonium ion.

# Chapter 2

# Porous Silica Materials

Porous materials are classified and defined by IPUAC by the size of the pores as, micro-, meso- or macroporous materials. The classification states that pores smaller than 20 Å are micropores, pores in the range 20 - 500 Å are mesopores and pores larger than 500 Å are macropores. Porous silica materials with micropores, zeolites, have a crystalline network, whereas mesoporous silica materials have an amorphous network. The following sections provides a brief description of the two materials and their respective structure directing agents, SDA, which are integral components in the synthesis. The last section describes the model systems designed to mimic the molecular behaviour of the silica and SDA at the initial stages of a synthesis of mesoporous materials.

### 2.0.1 Zeolites

The term zeolite was coined by the Swedish mineralogist Axel Fredrik Cronstedt in 1756 when he observed that the unknown mineral he was analysing frothed when heated over a flow-pipe flame.[1] It was water contained in the porous structure that vaporised. A number of zeolites occur naturally, but most of the known structures are synthetically made.

Zeolites are crystalline aluminosilicates, formed of tetrahedrons, either $AlO_4$ or $SiO_4$, where the tetrahedral atom is generally denoted as $T$. The tetrahedrons are linked via the oxygen in the corner of the tetrahedron. This results in a formula of $TO_2$. Zeolites with incorporated $Al^{3+}$ in the framework carry a charge, which is neutralised by incorporation of guest cations in the material. An all silica based material carry no charge since the silicon is tetravalent. Zeolites have well defined pore sizes (of-

ten characterized by the number of T-atoms in the ring defining the pore opening) due to its crystalline framework. These qualities make zeolites interesting materials for many applications such as molecular sieves, ion exchangers, absorbents, for catalysis, but also for more unconventional applications as blood-coagulants.[2]

The structure commission of the International Zeolite Association, has constructed a compilation of structures, which have been assign a three letter combination that defines the structure.[3] This three letter combination defines the structure, but not the ratio between silicon and aluminum atoms. Neither does it provide information regarding any guest molecules. The structure can be described using by sub units, so-called secondary building blocks that are repetitive units in the zeolite structure.

A normal route to synthesise zeolites is in an alkaline aqueous solution via a hydrothermal route,[4] and hence the reaction occurs at a high pressure and temperature. Water has been suggested to play many roles in hydrothermal synthesis, being the solvent, accelerating the reaction and some times participating in the reaction.[4] The alkalinity typically originates from addition of alkali-metal hydroxides. The pH value have been shown to affect the solubility of the Si/Al sources and the rate of polymerization of polysilicates and aluminate ions.[4] Organic cations, such as tetraalkylammonium ions, $TAA^+$ (see figure 2.1 and section 2.1.1), are efficient SDAs enabling the formation of many high Si/Al ratio zeolites.[4–6] The role of organic $TAA^+$ cations and their influence as partly hydropho-

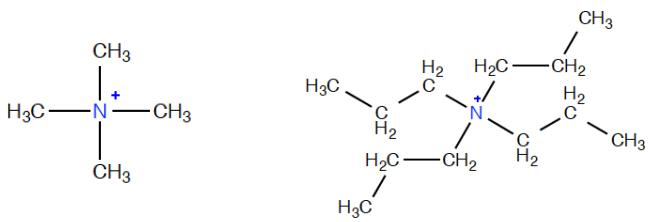

*Figure 2.1: Structures of two tetraalkylammonium ions, (left) tetramethylammonium, $TMA^+$, and (right) tetrapropylammonium, $TPA^+$.*

bic entities, have been discussed in synthesis of zeolites.[7] Experimentally it has been shown that tetraethylammonium ions, $TEA^+$ and tetrapropylammonium ions,$TPA^+$, have a large influence on the synthesis of sil-

ica MFI and BEA. The $TPA^+$ initiate nucleation and propagates growth, whereas the $TEA^+$ only propagates growth. The formation process is of interest and has been the subject of several investigations. An in-situ investigation of the formation of pure-silica zeolite ZSM-5 (MFI), or silicalite-1, in the presence of $TPA^+$, indicates that the hydrophobic $TPA^+$ benefits from sharing hydration shells with small silicates, and several of these aggregates will assemble into small primary units. The primary units are then suggested to aggregate and eventually form nuclei for crystal growth.[8] The pure-silica zeolite ZSM-5 (MFI), with $TPA^+$, has also been modelled, showing that the $TPA^+$ has two functions, stabilizing the large 10-membered ring and structuring itself in the channel intersections during and after aggregation.[9]

The formation of zeolites is a highly intricate process, controlled by several parameters, such as the pH, presence of different alkali-metal cations, the silica/alumina source and the presence of structure directing agents, such as tetraalkylammonium ions.

### 2.0.2 Mesoporous Silica

In the desire to produce porous silica material with pores larger than those in zeolites, a new material emerged in the early 1990. The material was formed using supramolecular structure directing agents, i.e. cationic surfactant assemblies, and had two dimensional (2D) hexagonal order, monodisperse pores in the meso-regime and an amorphous network of silica.[10] The scientific field of ordered mesoporous silica has since developed to also including materials synthesized with anionic[11] and non-ionic amphiphilic[12,13] SDAs. The first ordered mesoporous material, synthesised by Kresge *et al.*[10] , denoted MCM-41 (Mobil Composition of Matter), has the hexagonal structure just mentioned. With time the routes to synthesise mesoporous silica material developed, and so did the structures that were synthesised. Today, it is possible to synthesis a variety of different structures, such as 2D hexagonal[10,12,13] , bicontonious cubic,[14] lamellar[11,14] and some more unusual structures as for instance the tricontinuous hexagonal.[15] The structures reveal strong resemblance to the liquid crystalline phases found in amphiphile/water systems (discussed more in section 2.1.2).

The 2D hexagonally structured material can be synthesised in a variety of systems, where two common systems produce MCM-41 or SBA-

15. SBA-15 was first synthesised by Zhao *et al.*[12,13] in Santa Barbra using non-ionic polymers as SDAs in an acidic environment. MCM-41 is synthesized with cationic surfactants in an alkaline aqueous solution. The ever changing need to improve the materials for different applications have led to a range of synthesis routes, ranging from acidic to alkaline environments, with different silica sources and structure directing agents. One of the, today, more common silica sources is the tetraalkoxysilanes, see figure 2.2. When the tetraalkoxysilanes, e.g. tetramethoxysilane

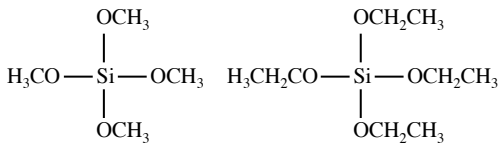

*Figure 2.2: Structures of tetramethoxyilane (TMOS) and tetraethoxysilane (TEOS).*

(TMOS) and tetraetyoxysilane (TEOS), are dissolved in water they hydrolyse and for one molecule that hydrolyse four alcohols are produced (methanol and ethanol, respectively, from TMOS and TEOS). This entails a presence of alcohol in the synthesis. Other frequently used silica sources are sodium silicates, which as the name suggests introduce sodium ions in the synthesis solution.

The simplest silica species, orthosilicic acid, $Si(OH)_4$ produced as the tetraalkoxysilanes hydrolyse, is a weak acid with a $pK_{a_1}$ of 9.8[16] and a $pK_{a_2}$ of 13.4.[17] Larger polysilicic species have $pK_a$ values smaller than those of orthosilicic acid.[16] Hence, silica species, present in a synthesis solution of mesoporous material in alkaline conditions, will typically be negatively charged.

Synthesis solutions for mesoporous silica materials, utilizing cationic SDAs, in an alkaline environement contains a variety of molecules. The SDA, frequently an alkyltrimethylammonium halide,[10,11,18–20] see figure 2.3, is dissolved in a aqueous alkaline solution, often with $NH_3$,[11,20,21] NaOH[11,18] or tetraalkylammonium hydroxide[19] as the base. In the case of sodium silicates the solution is inherently basic.[11] If an alkoxysilane is used as the silica source, the SDA is dissolved in an alkaline solution, to which the silica is directly added.[20,21] It has also been shown that addition of short chain alcohols can alter the structure; addition of methanol,

ethanol or propanol can change the structure from hexagonal to cubic to lamellar.[20] Mesoporous silica materials can hence be synthesized under a range of conditions.

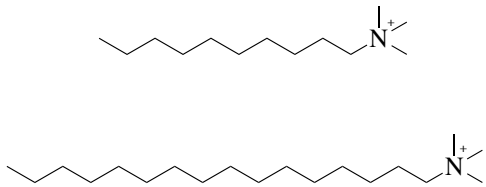

*Figure 2.3: Structures of two alkyltrimethylammonium surtactants; (top) decyltrimetylammonium with a 10 carbon long chain, $C_{10}TA^+$, and (bottom) cetyltrimethylammonium with a 16 carbon long chain $C_{16}TA^+$*

The first study of the formation mechanism of mesoporous materials suggested a liquid crystal templating scheme, where the cationic surfactant formed a hexagonal structure, around which the silica penetrated and polymerised.[14] This scheme was soon disputed due to the fact the materials could also be synthesised in solutions with low surfactant content, as long as spherical surfactant aggregates (micelles) were present. One mechanism, proposed by Monnier *et al.*,[22] taking into account that the SDA initially is in the form of spherical aggregates, suggests that small silica oligomers attach to the surfactant assembly. This will lead to screening of the charges at the surface of the SDA, due to the negative silica species, and a lamellar phase will form that subsequently corrugate into a 2D hexagonal phase as the silica condensate. Another proposed mechanism, by Zana, Frasch and co-workers,[23,24] involves the formation of small silica oligomers, which attract the oppositely charged surfactants and form a complex. As the silica oligomers grow they attract more surfactants from the micelles. This complex will eventually rearrange into a 2D hexagonal phase and precipitate. This theory originated from the fact that Zana, Frasch and co-workers couldn't find any evidence that silica species associated to the surface of the SDA aggregates. A third suggestion came from Hollamby *et al.*,[25] who investigated the formation of mesoporous silica particles using time-resolved small angle neutron scattering. The suggestion was that the silica oligomers adsorbed onto the SDA assemblies, causing several SDA-silica assemblies to form larger aggregates, in which the SDA rearranges as silica continues to polymerise. The common denominator of all suggested

mechanisms is the electrostatically based driving force between the negatively charged silicate species and the cationic SDAs.

The formation process is so fast when TEOS is used as a silica source that in-situ scattering measurements can hardly resolve the stages before the hexagonal phase is formed.[21,26] The hexagonal phase appears already within 80 seconds after the addition of TEOS.[21,26] As a consequence, alternative investigation methods have been applied to probe the formation process. This often involves a model system, which does not polymerise[23,24,27] One way to probe the interactions in the synthesis, using a model system, is to gradually increase the complexity of the system until the multi-component system is closely resembling the true system. By investigations of both the individual components' behaviour and the cooperative behavior, of SDA and silica, a more extensive portray, of the formation process, can be depicted.

## 2.1 Structure directing agent - SDA

As previously discussed structure directing agents, SDAs, are required in the formation process of porous silica materials. The SDAs become incorporated in the pores, or cavities, in the material as the formation proceeds. The SDAs are trapped in the material and have to be removed before the material become porous. As one of the crucial components in the synthesis, their behavior in aqueous solutions are of great interest. The coming two sections will therefore address their behavior in water, first the molecular SDAs, tetraalkylammonium ions, utilized in zeolite synthesis and then the supramolecular SDAs, cationic (alkyltrimenthylammonium) surfactant assemblies, applied in some mesoporous silica materials's synthesis.

### 2.1.1 Molecular SDAs

As discussed previously, the tetraaklylammonium ion ($TAA^+$), will influence the synthesis of zeolites. The $TAA^+$ ions have an inherent duality; they have a polar part and an apolar part. The $TAA^+$ also have an interesting symmetrical geometry with a polar centre, nitrogen, connected to four hydrocarbon groups, see figure 2.1. The length of the hydrocarbon groups have different effects on the formation process of zeolites, a fact that has been attributed to their difference in hydrophobicity. Hence,

their behaviour in aqueous solutions is interesting to understand.

Tetraallkylammonium ions have been probed with for instance neutron scattering,[28–32] NMR,[33,34] and computer simulations.[35–38] The interest have largely focused on whether the $TAA^+$ will start to form cation-cation pairs of aggregates due to increased hydrophobicity as the length of the hydrocarbon groups increase and if the water around the ions structure. Neutron scattering of aqueous $TAA^+$ solutions give little evidence of ion clustering and structuring (or de-structuring) of the water.[28–32] Molecular dynamics (MD) simulations of aqueous solutions of $TMA^+$ and $TBA^+$, at various concentrations, reveal little cation-cation aggregation.[35] However, Huang *et al.*[38] observed aggregation of the larger $TAA^+$ ions, using x-ray scattering and this was supported by their MD simulations. A change in the behaviour was observed between the $TEA^+$ (tetraethylammonium) and $TPA^+$; the larger cations formed clusters whereas the smaller $TAA^+$ ions remained free in solution. The simulations either revealed any large change in the structure of the water molecules around the ions.

Tetraalkylammonium ions normally have a halide ion (chloride or bromide) or a hydroxide ion as counterion. Solutions of TMACl, investigated with neutron scattering, showed that the chloride was almost fully hydrated, indicating that the counterion is not strongly associating to the $TAA^+$ ions.[28]

The $TAA^+$ ions appear to be both ions and hydrophobic entities, where the magnitude of the cationic character appears to be determined by the length of the hydrocarbon groups. The hydrophobic character would favour an interaction other hydrophobic entities. As silicate anions polymerise, the silica network becomes gradually more hydrophobic. This would indicate that the larger $TAA^+$ ions would benefit from interacting with the larger silica entities, whereas the smaller $TAA^+$ would preferentially interact with the smaller silicate anions due to electrostatic interactions. However, the range at where the electrostatic interactions are relevant will be greatly affected by the presence of the charged silicate anions, compared to the pure aqueous solutions. The presence of silicates will increase the ionic strength, as they are typically anions at high pH. An increase in ionic strength will impede the electrostatic interactions.

### 2.1.2 Supramolecular SDAs

The supramolecular SDAs are aggregates of amphiphilic ions, in this case cationic surfactants: alkyltrimethylammonium ions (figure 2.3). Alkyltrimethylammonium ions have a polar, charged, headgroup and an apolar carbon tail. The charged headgroup is easily solvated in an aqueous solution, whereas the hydrophobic carbon tail have limited solubility. The interactions between the molecules are governed by two opposing forces, which will result in a self-assembly of the molecules at a given concentration. This concentration is the *critical micelle concentration*, CMC. The positive interaction between the carbon tails is the attractive component in the self-assembly process. Forces counteracting the self-assembly process results from the packing of the charged headgroups (and the subsequent loss in entropy originating from the fact that the molecules are no longer free to move around, randomly, in the solution). The self-assembly will therefore result in the heagroups being as far apart as possible. This is a start-stop process and the assemblies formed will be monodisperse. A common way to express the balance between the hydrophobic chain and the charged headgroup is with the surfactant packing parameter, $N_S$:[39,40]

$$N_S = \frac{v}{a_0 l} \tag{2.1}$$

where $v$ is the volume of the hydrocarbon tail, $a_0$ is the effective headgroup area and $l$ is the length of the hydrocarbon tails. If this parameter is $1/3$, spheres are formed (micelles). $N_S = 1/2$ gives cylinders and $N_S = 1$ gives planar surfaces. These different shapes can be packed into structures, to maximise the distance between them, which is beneficial as the charges will then be as far apart as possible. A common structure for the alkyltrimethylammonium ions (carbon length of 10-16), in an aqueous solution, at low concentrations is an isotropic solution of micelles. As the concentration increases the micelles will elongate to eventually become rods, or cylinders that pack in a hexagonal phase. With further increase of the surfactant concentration a cubic phase is typically obtained and at even higher concentrations a lamellar phase will form, see figure 2.4.[41] These structures are similar to the structures found in mesoporous silica materials as previously mentioned. As the structures change, the effective headgroup area $a_0$ will decrease. This causes a decrease in the curvature of the structure and explains the transformation between the different phases. The size of the micelle is highly dependent

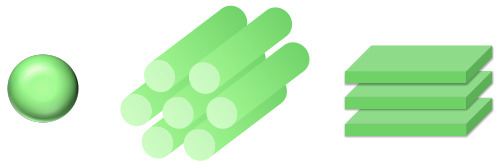

*Figure 2.4: Illustrations of different phases common in the surfactant water systems. From left to right: micelles, the hexagonal phase and the lamellar phase.*

on the length of the carbon tail, $l$, which in its extended state can be expressed as:

$$l = 1.5 + 1.27n_c \tag{2.2}$$

where $n_c$ is the number of carbons in the chain. 1.5 is due to the size of the terminal methyl group (van der Waals radius of 2.1 Å) minus of half the bond length of the atom not included in the hydrocarbon chain (0.6 Å). 1.27 is the projection of the carbon-carbon distance for a chain in all trans configurations.[40] This length will be approximately the largest radius of the hydrophobic core that a spherical micelle can form. Due to the packing of the headgroups and the limited size of the hydrophobic core, the number of surfactants in each micelle will be approximately the same. This number is called the aggregation number, $N_{agg}$.[39,40]

The identity of the counterion has a major influence on the micelle properties. Alkyltrimethyalammonium surfactants often have a halide ion as a counterion. The effective headgroup area, $a_0$, will be affected by the screening from counterions associated to the micelle surface. If the counterions are highly associated to the surface, $a_0$ will decrease, and the micelles will grow in size. From an electrostatic point of view a divalent ion should bind stronger than a monovalent ion to the micelle surface.[42,43]

An effect of the counterion has been observed for cetyltrimethylammonium, $C_{16}TA^+$ system with bromide, chloride, sulphate, nitrate, fluoride as counterion when probed with isothermal titration microcalorimetry and conductivity. Both the size and counterion association was different.[44] With increased screening of the headgroups, due to a higher degree of counterion association, the micelles start to grow and at a given point elongate. The formation of elongated, threadlike, micelles have been observed with para-Toluene sulphonate (p-TS) as counterion.[45] Ap-

parently the self-assembly characteristics are highly dependent on which counterion that is present. The identity of the counterion determines the degree of association to the micelle surface, i.e. the different anions bind more or less strongly to the micelle. This is typically connected to the Hofmeister series, which is an experimentally determined series for ions affinity to a surface (originally a protein). The suggested order of the series, for anions, is as follows:[40,46]

$$SO_4^{2-} < OH^- < F^- < Cl^- < Br^- < NO_3^- < I^-$$

The explanation for this ion-specific effect is a still ongoing discussion,[46–49] and is out of the scope of this work.

The counterion association is an important factor in the properties of the micelle. The counterion association have been shown to be almost unaffected by the surfactant concentration,[39] but highly dependent on the temperature.[50,51] The counterion association can also be altered by the addition of alcohols.[52] However, alcohol also influence the cmc of ionic micelles.[39,52] The dressed micelle model, designed to asses the counterion dissociation, has been formulated by Evans, Mitchell and Ninham,[53] and was later modified by Hayter.[54] This model assesses the counterion association from measurable parameters, as for instance cmc and micelle size.

The self-assembly characteristics, such as he cmc value, are affected by additions of salt as the ionic strength of the solution increases. Simple salts, for instance NaBr, screen the electrostatic interactions and decrease the effective headgroup area, decreasing the repulsive force in self-assembly process.[39,55]

The micelle properties are highly dependent on additions of both salt and alcohol, as well as temperature and counterion. These are all factors that are important parameters in the formation of mesoporous silica, like MCM-41. The synthesis solutions have high ionic strengths, resulting from negative silica species due to high pH, hydroxide groups, possible additions of sodium from the silica source, etc. If tetraalkoxysilanes iare used as the silica source alcohol is produced, which is another factor that influences the SDA.

## 2.2 The model system

The desire for rational design have motivated many investigations to unravel the mechanisms behind the formation of both zeolites and mesoporous material. A model system was designed to allow an investigation of the early stages of a synthesis. In order to facilitate the interpretation of the underlying driving forces the model systems was first probed with its individual components, before an investigation was performed on the more complex system.

The structure directing agents probed are TMABr and TPABr, which functions as SDAs in zeolite syntheses, and decyltrimethylammonium micelles, with various counterions, see figure 2.5, functioning as SDAs in mesoporous silica materials.The different counterions are expected to influence the behaviour of the SDA. The behavior of both monovalent and divalent ions was investigated, as well as the degree of counterion association. The systems are all probe at room temperatures (25°C). The concentrations of the SDAs, were set at 0.4 M, providing a substantial signal in scattering techniques. The cationic surfactant, $C_{10}TA^+$, is at these concentrations considered to spherical micelles, based on the phase diagram of the aqueous $C_{10}TABr$ system.[41]

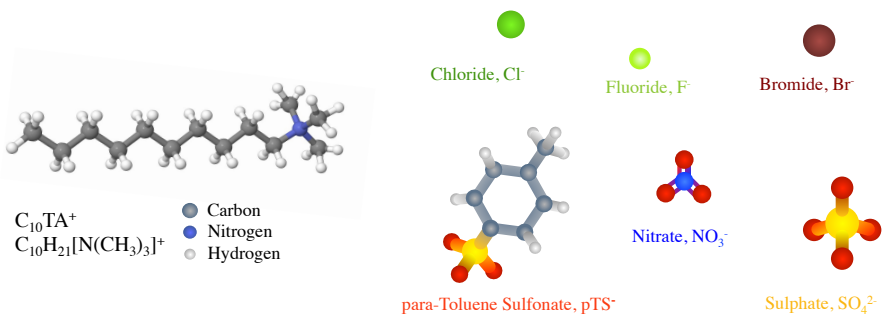


*Figure 2.5: Illustrations of the $C_{10}TA$ and the investigated anionic counterions.*

A cubic octamer, $Si_8O_{20}^{8-}$ (figure 2.6), with 8 $TMA^+$ as counterions, was chosen to represent the silica species early in the synthesis. This cubic octamer is stable in aqueous solutions as it does not polymerise. This model silica species is investigated on its own in aqueous solutions,

and together with different additives relevant for a synthesis of porous silica materials. The behaviour of the silica model is examined using $^{29}$Si-NMR. The SDAs are first probed individually in aqueous solutions,

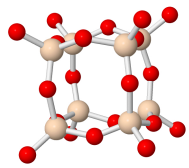

*Figure 2.6: The cubic octamer, chosen to represent the silicate anions present in the early stages of the synthesis of MCM-41.*

before the system composed of both $C_{10}$TABr and the silica model is investigated. The concentrations of the SDA remains the same (0.4 M) and two different concentrations of the silica model is probed.

The model systems are typically investigated using wide and intermediate angle neutron scattering, coupled with empirical potential refinement modelling and the silica species are monitored with $^{29}$Si-NMR. See chapter 3.3 for more information regarding the different techniques.

# Chapter 3

# Methodology

## 3.1 Nuclear Magnetic Resonance Spectroscopy

The following section will give a brief introduction to Nuclear Magnetic Resonance, NMR, Spectroscopy. For a more in depth description see for instance references 56, 57. NMR, spectroscopy exploits the fact that specific nuclei possess an inherent magnetic property; spin angular momentum, commonly denoted as *spin*. The spin will orient, in a few allowed states, when subjected to an external magnetic field. The energy difference between these states, ΔE, depends on both the nuclei and the magnitude of the external magnetic field, $B_0$. By subjecting the nuclei to an alternating electromagnetic field the spin can flip from a low energy state to a higher energy state. This happens if the electromagnetic field oscillates with a specific frequency ($\nu$) which satisfies the resonance condition;

$$\Delta E = h\nu \tag{3.1}$$

where $h$ denotes Planck's constant. It is ΔE that is measured with NMR. The frequency is given by the Larmor frequency:

$$\nu = \frac{\gamma B}{2\pi} \qquad (or\ \omega = \gamma B) \tag{3.2}$$

where, $\gamma$ is the gyromagnetic ratio, sometimes described as a measure of a nucleus inherent magnetic property, and $B$ is the magnitude of magnetic field experienced by the nucleus. $\omega$ denotes the angular frequency.

One of the major advantages of NMR spectroscopy is the fact that although the spin is sensitive to the surroundings, it only weakly interacts

with the surroundings. This sensitivity affects the resonance frequency, and this is the origin of chemical shift, $\delta$. The chemical shift is normally not assigned an absolute value but is quantified relative to a references frequency, $\nu_{ref}$;

$$\delta = 10^6 \cdot \frac{\nu - \nu_{ref}}{\nu_{ref}} \tag{3.3}$$

The chemical shift allows for differention between the same type of nuclei within one molecule (provided that they are not magnetically equivalent).

Spin is measured in quantities of $\hbar$ ($\hbar = h/2\pi$) as $[I(I+1)]^{1/2}\hbar$, where $I$ is the nuclear spin quantum number. $I$ can have values of 0, 1/2, 1, 3/2... where $I$ larger than 4 is uncommon. A quantum number of 0 means that the nucleus gives no signal in NMR: examples are $^{12}$C, $^{16}$O and $^{28}$Si. The isotopes with spin 1/2 can only change between two energy states when subjected to a magnetic field. From here on, the only nuclei discussed will be those with spin 1/2.

The difference in distribution between the two states is small, since $\Delta$E is small in comparison to $kT$ ($k$ is the Boltzmann constant, and T is the temperature), and hence NMR is a fairly insensitive spectroscopy method. The signal from the sample becomes stronger with increasing magnetic field, see equation 3.1 and 3.2, but also with increasing gyromagnetic ratio, $\gamma$, and the number of nuclei that contributes to the signal. This facts make the $^1$H a sensitive nucleus in NMR, while $^{29}$Si (table 3.1) is a considerable weaker nucleus.

*Table 3.1: Parameters for the $^1$H and $^{29}$Si subjected to a 11.5 T magnetic field.*

| isotope | $I$, *spin* | $\gamma$ [MHz rad T$^{-1}$] | $\nu$ [MHz] | Natural abundance % |
|---|---|---|---|---|
| $^1$H | $\frac{1}{2}$ | 26.75 | 500 | 99.98 |
| $^{29}$Si | $-\frac{1}{2}$ | -5.32 | 99.6 | 4.7 |

The applied external magnetic field will cause the sample to have a net magnetization, $M_0$, in the same direction as the applied field,

normally denoted the z-direction. A spin will precess around the z-direction,$\vec{M}$, (figure 3.1) at an angular frequency of $\omega$. A spectrum is recorded by applying a magnetic pulse, $\vec{B}_1$, that rotates the direction of the net magnetization over a specified angle with respect to the z-axis, (the angle depends on the duration of the pulse). A 90° pulse will flip the net magnetization into the x-y-plane. After the pulse, the spins will precess in the x-y plane, and will slowly relax back into the z-direction. It is therefore important that all nuclei have time to relax back into the z-direction before applying a second pulse (figure 3.1). In order to increase the signal-to-noise ratio several consecutive pulses are recorded. The oscillating signal from the sample will decay with time as the spins align back into the z-direction, which is recorded, as a free induction time (FID). The FID is Fourier transformed from the time domain into the frequency domain, and a frequency spectrum is obtained. There are in general two relaxation processes; one along the z-axis with a time constant $T_1$ and one in the x-y plane with the time constant $T_2$.

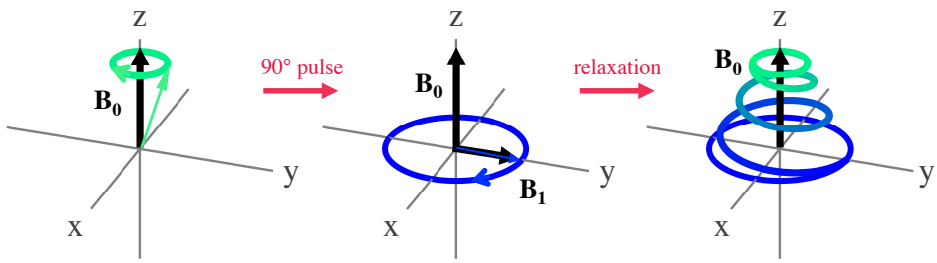


*Figure 3.1: Schematic illustration of a 90° pulse, which describes how one spin will process around the z-axis.*

The effect of the low sensitivity of the $^{29}$Si atom compared to the $^{1}$H is illustrated in figure 3.2. Note that the $^{1}$H spectum is obtained a considerably shorter time than the $^{29}$Si spectrum, see figure caption for more details.

Another aspect influencing the NMR signal, is spin-spin couplings, which gives rise to peak splittings originating from a splitting of the

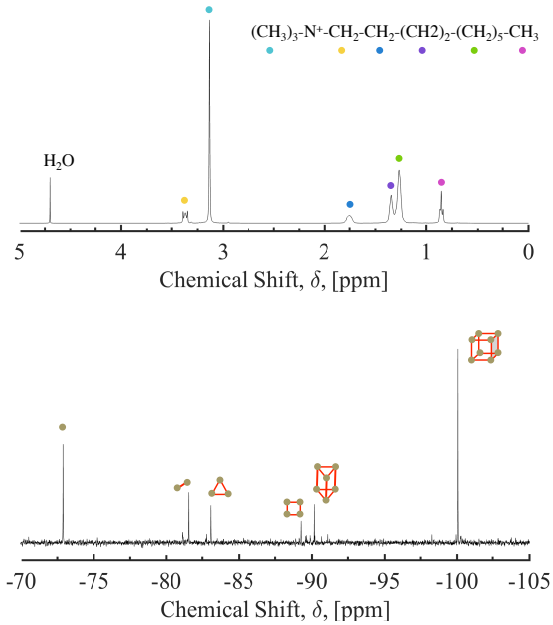


*Figure 3.2: Two different NMR spectra; (top) $^{1}H$ spectrum of $C_{10}TABr$ in $D_2O$, (bottom) $^{29}Si$ spectrum of a silica salt solution (18wt%). The different hydrogens in the surfactant have been marked in the spectra, and an example of peak splitting can be seen at the pink dot. The different silica species are marked in the spectrum, with silicon atoms marked as beige dots, all linked by oxygens. The $^{1}H$ spectra has been recorded for a few seconds (16 pulses), whereas the the silicon spectra has been recored for over 3 hours (128 pulses). The concentration of the protons are much higher than that of the silicon atoms; one surfactant molecule contains 21 protons whereas the largest silica specie only contain 8 Si atoms. This will also contribute to the difference in the signal-to-noise between the two spectra.*

allowed energy states. It is possible to suppress peak splitting by subjecting the sample to a magnetic pulse with a selective frequency. This is called decoupling.

## 3.2 Neutron diffraction

Scattering is a non-invasive and versatile technique which can be used to probe objects in solution of varying size. The wavelength of the irradiating beam determines the size of the objects which can be probed. Both x-rays and neutrons therefore probe samples down to the Ångström

length scale, whereas light probe objects at the nanometer to micrometer range. This makes neutrons and x-rays suitable to probe even at an atomistic level. Hence, the coming section will provide an overview of neutron scattering, where a more elaborate description can be found elsewhere.[58,59]

The incoming radiation is normally a plane-wave, with the propagation vector, $\vec{k_i}$ and a magnitude of $2\pi/\lambda$, where $\lambda$ is the wavelength of the incident wave. A convenient way of expressing the difference between the incident and scattered wave is with the scattering vector $\vec{Q}$, see figure 3.3.

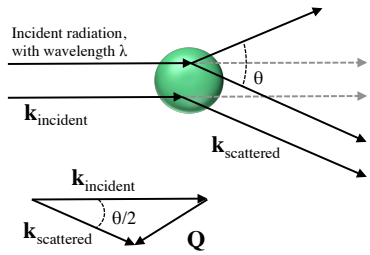


*Figure 3.3: Schematic illustration of a scattering event, where the incident beam scatters into the angle $\theta$. The scattering vector $\vec{Q}$ (or $\mathbf{Q}$), is described by the propagation vectors of the incident and scattered beam.*

This is based on the assumption that the scattering is so weak that most of the incoming waves passes trough the sample without deviation and if it scatters it only occurs once, and that the incident wave is not distorted by the scattering medium. This would imply (quasi-)elastic scattering; the wavelength remains unchanged. The sample is also assumed to be isotropic and ergodic. With these assumptions the amplitude of the propagation vectors of the incident and scattered wave will then be the same, and the amplitude of the scattering vector, can be expressed as:

$$|\mathbf{Q}| = Q = \frac{4\pi}{\lambda} \sin\frac{\theta}{2}. \tag{3.4}$$

where $\theta$ is the scattering angle, see figure 3.3.

The measured quantity in a scattering experiment is the differential scattering cross section: $d\sigma/d\Omega$, which is a measure of the fraction of the beam being scattered into the solid angle $\Delta\Omega$. The differential scattering cross section, if normalised per atom, can be expressed as:

$$I(Q) = \frac{1}{N}\left\langle \sum_{i=1}^{N}\sum_{j=1}^{N} b_i b_j \mathrm{e}^{(-i\mathbf{Q}\cdot(\mathbf{r_i}-\mathbf{r_j}))} \right\rangle \tag{3.5}$$

where $N$ is the number of atoms in the system, $b$ is the scattering length of atom $i$, $\mathbf{Q}$ is the scattering vector and $\mathbf{r}$ is the position vector of atom $i$. The angle brackets denote the ensemble average and if, as previously mentioned, the sample is isotropic and ergodic equation 3.5 can be simplified, and expressed in terms of the site-site radial distribution functions, $g_{\alpha\beta}$. Equation 3.5 can the be written as:

$$I(Q) = I_{self}(Q) + I_{distinct}(Q) \tag{3.6}$$

and

$$I_{self}(Q) = \sum_{\alpha} c_\alpha \langle b_\alpha^2 \rangle \tag{3.7}$$

where $c_\alpha$ is the atomic fraction and $\langle b_\alpha \rangle$ is the spin and isotope averaged scattering length density of atom $\alpha$. The self-scattering is assumed to be a Q-independent constant. The distinct-scattering can be divided into two terms: the intra-molecular and inter-molecular. The intra-molecular term only describes the scattering from atom pairs on the same molecule, while the inter-molecular term describes the scattering between two atom types on different molecules. The distinct scattering term can be expressed as:

$$I_{distinct}(Q)) = \sum_{\alpha,\beta\geq\alpha} (2-\delta_{\alpha\beta}) c_\alpha \langle b_\alpha \rangle c_\beta \langle b_\beta \rangle S_{\alpha\beta}(Q) \tag{3.8}$$

where $S_{\alpha\beta}$ is the partial structure factor between atom types $\alpha$ and $\beta$, and can be expressed as;

$$S_{\alpha\beta}(Q) = \frac{4\pi\rho_0}{Q}\int_0^\infty r(g_{\alpha\beta}-1)sin(Qr)\mathrm{d}r \tag{3.9}$$

where $\rho_0$ is the atomic number density of the sample. The radial distribution function, $g_{\alpha\beta}(r)$, will provide us with spatial information about the system, i.e. how atoms $\alpha$ and $\beta$, on different molecules, correlate to each other as function of the distance, $r$. The inter-molecular term of the

distinct scattering term can be expressed as equation 3.8, but then the structure factor and radial distribution function will only describe the correlations between different atom types on different molecules. These equations can be expressed in the same manner for molecules, as scatterers, but using the concentrations, densities and $N$ for the individual molecules rather than the atoms.

The structure factor describes the correlations in the system between $\alpha$ and $\beta$, and will be 1 if no correlations existed in the system, as for a dilute system of micelles, which are too far apart to "feel" each other. However, if probing something at the atomistic level (contributing to the diffraction curve at intermediate angles, see left-hand side of figure 3.4) the correlations between the scatterers would alway be present. Micelles, being much larger than atoms, will contribute to the diffraction curve at smaller Q values, see righthand side of figure 3.4.

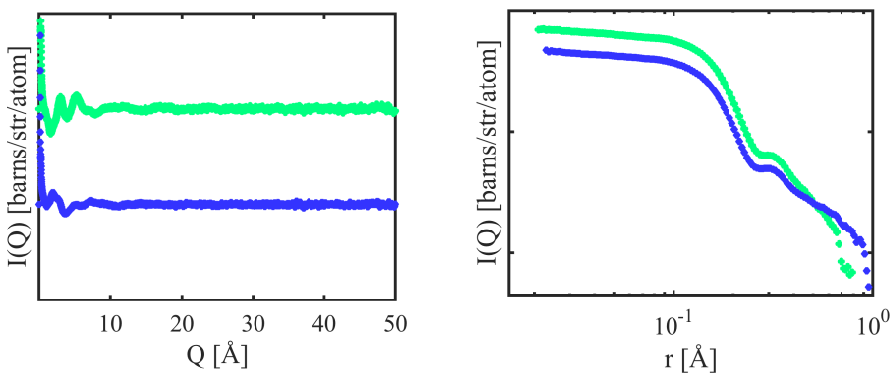


*Figure 3.4: The scattering pattern of a 0.4M $C_{10}$TABr with 22 wt% silica salt. Left: displayed on a linear scale for near to intermediate Q-range. Right: displayed on a logarithmic scale for low Q-values, highlighting the micelle contribution.*

One of the compelling arguments for using neutron scattering is the possibility to accentuate different parts of an investigated sample by isotope substitution.[60] Isotope substitution allows us to examine different atomic pair correlations by taking advantage of the fact that isotopes frequently have different scattering lengths.[61] It is presumed that isotope substitution does not alter the structure of the investigated system, which is the case for many systems. A systematic exchange of all atomic species would promote a complete extraction of all pair correlations, a

complete structure determination. As a consequence in the often large and complex systems investigated it becomes impossible to exchange all atomic species. Unfortunately there are also only a few substitutions which are practically achievable, for reasons of cost and isotope availability. One frequently practiced isotope substitution is that of hydrogen (H) with deuterium (D). These isotopes have exceedingly different scattering lengths and are in many systems known to not cause any significant alterations of the underlying structure. This substitution is often powerful enough to determine the physical and chemical properties of a system by providing critical insight into important inter-molecular correlations.[62]

Scattering suffers from drawbacks in the loss of phase as well as limited choice of isotope substitution. As a consequence to this there is a prerequisite of a certain degree of knowledge about the sample when interpreting the data. Normally a model is fitted to the measured data in order to gain information about the sample.

## 3.3 Empirical Potential Structure Refinement - EPSR

One way to interpret scattering data is through models, using for instance Empirical Potential Structure Refinement (EPSR).[63–66] EPSR is a type of reverse Monte Carlo (RMC) simulation,[67] which like RMC applies an additional constraint to the simulation, that of experimental data. However, EPSR uses, unlike RMC, a harmonic potential to describe the molecule. This harmonic potential used to describe the molecules is defined as:

$$U_{intra} = C \sum_{i} \sum_{\alpha\beta>\alpha} \frac{(r_{\alpha_i\beta_i} - d_{\alpha\beta})^2}{2w_{\alpha\beta}^2} \tag{3.10}$$

where $d_{\alpha\beta}$ is the average distance between atom $\alpha$ and $\beta$, $r_{\alpha\beta}$ is the actual distance between the two atoms in molecule $i$ and $w_{\alpha\beta}$ a width:

$$w_{\alpha\beta}^2 = \frac{d_{\alpha\beta}}{\sqrt{\frac{M_\alpha M_\beta}{(M_\alpha + M_\beta)}}} \tag{3.11}$$

where $M$ is the mass of atom $\alpha$ and $\beta$, respectively. The constant $C$ in equation 3.10 is determined by a comparison of the simulated structure factors with the data at high Q values.

The potential energy in EPSR has mainly two contributions, the reference potential ($U^{Ref}$) and the empirical potential ($U^{EP}$). These contributions can be divided into components that describe the contribution from each atom pair, at a distance $r$ apart ($U_{\alpha\beta}(r_{ij})$). The reference potential consists of, in addition to the harmonic potential describing the intramolecular energy of the molecules, a Lennard-Jones potential, an effective Coulomb contribution (if any charged species exists in the system), and an repulsive term:

$$U_{\alpha\beta}(r_{ij}) = 4\varepsilon_{\alpha\beta}\left[\left(\frac{\sigma_{\alpha\beta}}{r_{ij}}\right)^{12} - \left(\frac{\sigma_{\alpha\beta}}{r_{ij}}\right)^{6}\right] + \frac{q_\alpha q_\beta}{4\pi\epsilon_0 r_{ij}} + C_{\alpha\beta}\exp\left(\frac{1}{\gamma}(r_{\alpha\beta} - r_{ij}\right) \tag{3.12}$$

where $C_{\alpha\beta}$ is adjusted separately, preventing atoms $\alpha$ and $\beta$ to come closer than $r < r_{\alpha\beta}$. The hardness of the repulsive trem is controlled by $\gamma$, which is normally set to 0.3 Å. The Lorentz-Bertolt rules are used to combined the individual atom parameters to the mixed well depth parameter, $\varepsilon_{\alpha\beta}$, and range parameter, $\sigma_{\alpha\beta}$. The reference potential has no correction for long range effects, but is truncated with different functions depending on the contributions to it. The non-Coulomb part of the reference potential is truncated via:

$$T(r) = \begin{array}{ll} 1 & r < r_{minpt} \\ 0.5\left(1 + \cos\pi\left(\frac{r - r_{minpt}}{r_{maxpt} - r_{minpt}}\right)\right) & r_{minpt} < r < r_{maxpt} \\ 0 & r > r_{maxpt} \end{array} \tag{3.13}$$

The values of $r_{minpt}$ and $r_{maxpt}$ determine where the truncation reaches values below one and becomes zero, respectively. The Coulomb part of the reference potential truncates via:

$$T_C(r) = \mathrm{erfc}\left(\frac{r}{\sigma_C}\right) \tag{3.14}$$

where $\sigma_C$ is a width parameter.

The empirical potential attempts to create a potential that is based only on the difference between the experimental data and the simulation. It is described by a power series as:

$$U^{EP}(r) = kT\sum_i C_i p_{n_i}(r, \sigma_r) \tag{3.15}$$

where

$$p_{n_i}(r,\sigma_r) = \frac{1}{4\pi\rho\sigma^3(n_i+2)!}\left(\frac{r}{\sigma_r}\right)^n_i \mathrm{e}^{-r/\sigma_r} \tag{3.16}$$

and $\sigma_r$ is another width function, $C_i$ is a real number and $\rho$ is the atomic density number of the modeled system. A group of $r$ values are set and $n_i$ becomes:

$$n_i = \frac{r_i}{\sigma_r} - 3 \tag{3.17}$$

such that the range of the empirical potential becomes sensible for the investigated system. The function $p_{n_i}(r,\sigma_r)$ has an exact three-dimensional Fourier transformation, $P_{n_i}(Q,\sigma_Q)$, which allows for a direct estimation of $C_i$ from the experimental data by fitting the series:

$$U^{EP}(Q) = \sum_i C_i P_{n_i}(Q,\sigma_Q) \tag{3.18}$$

where $n_i$ is produced in an equivalent way to equation 3.17. This would imply that the $n_i$ have the same value as in equation 3.17, however, another smoothing is applied to the empirical potential, via $\sigma_r = 4\sigma_Q$. This will effectively smoothen the empirical potential.

There are in principle four different moves in EPSR: molecule translation, molecule rotation, rotation of any side groups (if defined) and movement of individual atoms within the molecule.[63–66] The acceptance of these moves are based on the Metropolis conditions, if the change in potential energy ($\Delta U$) is smaller than zero and the move is accepted, however if it is positive the move will be accepted with the probability of $\mathrm{e}^{-(U_{intra}+\frac{U^{Ref}}{kT}+\frac{U^{EP}}{kt})}$. This will result in each molecule having an individual geometry, whose move is not weighted by the thermal $kT$.

The diffraction data, $D(Q)$, from $M$ datasets are fitted in EPSR as the weighted sum over all atom pairs relevant to to the simulated partial structure factors as:

$$D_i(Q) = \sum_{j=1,N} w_{i,j} S_j(Q) \tag{3.19}$$

where $D_i(Q)$ represents the $i$ th dataset and the index $j$ runs over the number of partial structure factors, $N$. $N$ is defined by the number of atomic components, $x$, present in the model, as $N = x(x+1)/2$. The weights matrix is defined as $w_{ij} = (2-\delta_{\alpha\beta})c_\alpha\langle b_\alpha^{(i)}\rangle c_\beta\langle b_\beta^{(i)}\rangle$. Since the system is underdeterimed, due to as previously mentioned a shortage of

possible isotope substitutions, the inversion of $w_{ij}$ have to be resolved in order to generate a perturbation to each site-site potential. A confidence factor, $f$, is chosen so that a modified version of the weights can be expressed as $w'_{ij} = fw_{ij}$ for $1 \leq i \leq M$ and $w'_{ij} = (1-f)\delta_{i-M,j}$ for $M < i \leq (M+N)$. This means that the data is accepted with the confidence of $f$ and the simulation with $(1-f)$, given that $f$ is smaller than one. The inversions of the matrix can be used to produce the difference coefficient $C$ in equation 3.18, originating from the difference between the data and fit, which is used to produce the empirical potential. As the operations proceed the difference coefficient, $C$, will either become so small that the EP does not change any more or it reach a predefined limit (chosen for each system). At this point ensemble averages can be extracted from the simulation and provide information about the system.

This constitutes the base for the EPSR modeling, although many more options, potentials, constraints and calculations can be performed. For a total description of EPSR's capability and limitations, see references 63–66, 68.

## 3.4 Conductivity

A solutions ability to conduct an electric current can be assessed with conductivity. This is a measurement of the AC resistance, $R$, in a solution between two electrodes.[69] The specific conductivity, $\kappa$, can be expressed as[40] :

$$\kappa = \frac{k}{R} \qquad \left({}^{mS}/_{cm}\right) \tag{3.20}$$

where $k$ is a cell constant relating the distance between the electrodes, and the area of the electrodes via a solution of know resistivity. The conductance can also be expressed as the specific conductance ($^{mS\ cm}/_{mol}$), $\Lambda$,[40,69] which at low concentrations is proportional to the $\sqrt{c}$, where $c$ is the concentration. The change in conductivity, with increasing surfactant concentration, can be used to determine the cmc.[39,40] By fitting two linear relations to the conductivity, $\kappa$ vs $c$, the cmc will be determined as the intersect of the two linear relations, see figure 3.5. The change in specific conductivity can also be used to assess the counterion dissociation, $\beta_{mic}$, to the micelles.[70] The counterion dissociation can be estimated from the change in slopes, $k = {}^{d\kappa}/_{dc}$, for the two linear fits before and after

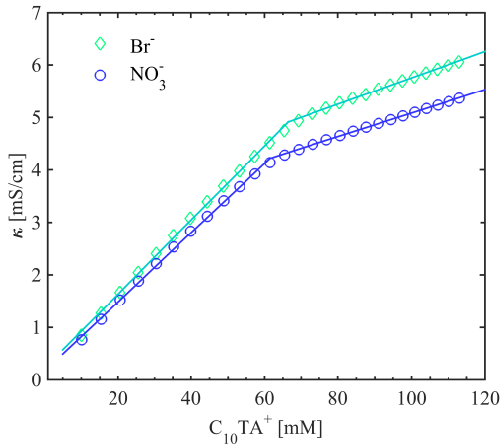


*Figure 3.5: The specific conductance of $C_{10}TABr$ (green) and $C_{10}TANO_3$ (blue) as a function of the concentration, the data is represented with symbols and the linear fits before and after cmc are displayed as lines. From the change in slopes it becomes apparent at which concentration micellisation occurs, and that $C_{10}TA^+$ forms micelles at lower concentrations with nitrate as counterion compared to bromide.*

micelliasation:

$$\beta_{mic} = \frac{k_{after}}{k_{before}}. \tag{3.21}$$

This will provide information regarding the counterions affinity for the surface, and provide insights into the difference in ion-specific effects between different counterions.

# Chapter 4

# Main results

In the formation process of porous silica materials a multitude of species are present in the aqueous solution. The main components are the structure directing agents (SDAs) and the silica source, which will polymerise and from the network around the SDAs. In order to disentangle the interactions taking place during the cooperative self assembly process, we have created systems focusing on the individual components in aqueous solutions. The systems contain silica species or SDAs. Also solutions containing both silica species and SDAs was probed. This gradual increase i the systems' complexity aim to provide insight into the behaviour associated to the two most relevant species in the formation process.

The results presented here is a selection of the principal results reported in papers I-IV. The results imply that the silica oligomers' interaction with the SDAs is an intricate process easily affected by the presence of other constituents in system. However, parts of the complex set of interactions taking place during a formation process starts to be unraveled. The gradual increase in the probed systems complexity shows that the SDA aggregates undergo a substantial change in the presence of silicate anions.

## 4.1 Small silica oligomers in aqueous solutions

The model silica oligomer, the cubic octamer (D4R), is unable to retain its structure in aqueous solutions. With $^{29}$Si NMR spectroscopy it is possible to quantify a fragmentation of the cube, which rapidly occurs when mixed with water. Typical $^{29}$Si NMR spectra, displayed in figure 4.1,

reveal distinct peaks from which the identity and abundance of the fragments can be determined. The cube undergoes hydrolysis and fragments

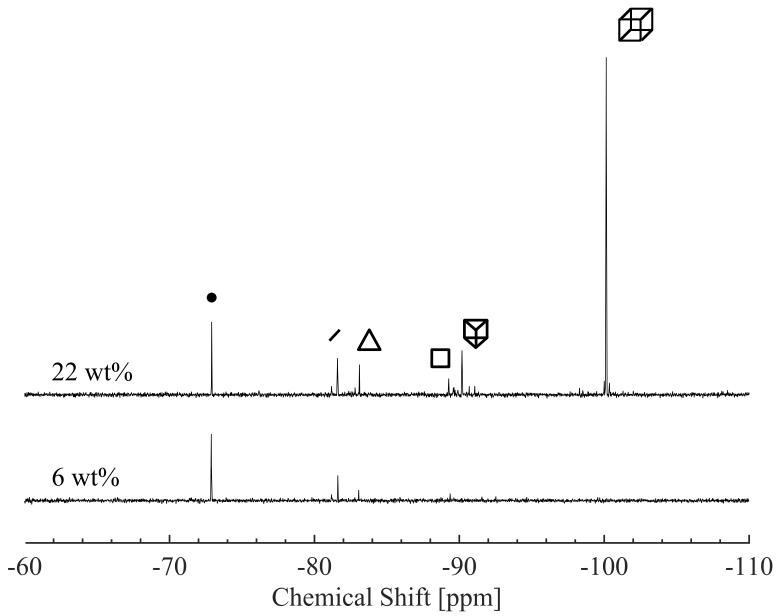


*Figure 4.1: $^{29}Si$ NMR spectra for two different silica salt concentrations, displayed relative to tetramethylsilane,TMS, ($\delta = 0$), revealing the concentration dependence on the fragmentation.*

into principally 5 other species: the monomer, dimer, single-3-ring (S3R), single-4-ring (S4R) and the double-3-ring (D3R), all depicted in figure 4.2, along with the cubic octamer.

All six species have previously been observed in silicate anion solutions[16,71–79] and during the synthesis of silica nanoparticles.[80,81] As the silica salt is mixed with water, at neutral pH, an increase in the pH value is concurrent to the fragmentation of the D4R, see table 4.1. All the silicate species present in the solutions are weak acids, and if the cubic octamer starts to protonate in solution the pH value will increase, due to the following reaction:

$$Si_8O_{20}^{8-} + 8\,H_2O \rightleftharpoons Si_8O_{12}(OH)_8 + 8\,OH^-$$

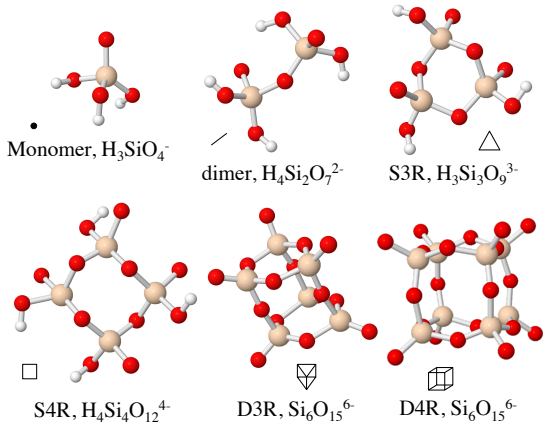


*Figure 4.2: The six most abundant species present in the silica solutions, Si atoms are depicted as beige spheres, oxygens as red spheres and hydrogen in white, together with their schematic illustration used to assign the resonance peaks in the $^{29}$Si-NMR spectra in figure 4.1*

*Table 4.1: The reaction between pH and increasing silica salt concentration.*

| Conc. silica salt [wt%] | Conc. Si atoms [M] | pH value |
|---|---|---|
| 3 | 0.096 | 11.53 |
| 6 | 0.195 | 11.85 |
| 12 | 0.390 | 12.11 |
| 18 | 0.585 | 12.26 |
| 22 | 0.739 | 12.32 |
| 28 | 0.928 | 12.34 |

An increase in pH will also be observed if the cube fragments into 8 monomers ($Si(OH)_4$):

$$Si_8O_{20}^{8-} + 20\,H_2O \rightleftharpoons 8\,Si(OH)_4 + 8\,OH^-$$

The monomer, or orthosilicic acid, has a $pK_{a_1}$ of 9.8[16] and a $pK_{a_2}$ of 13.4[17] and will therefore have gone through a first protonation step in the solutions. The larger polysilicic acid have lower $pK_a$ values than the monomer.[16] Based on this all of the different species will have gone through a first protonation step.

### 4.1.1 Tuning the stability of the cubic octamer

The stability of the cube can be tuned by either changing the concentration of sililca salt or by additions to the solutions of sodium salts, tetralkylammonium salts or short chain alcohols. The stability of the D4R and the fragments, as a function of increasing silica salt, was quantified using $^{29}$Si-NMR, see figure 4.3. A clear increase in the cube concentration with increasing Si-concentration is observed. A similar phenomenon has previously been observed in syntheses of the cube, where no cube was formed below a concentration of 0.3M $SiO_2$ (a concentration between the 6 and 12 wt% solutions).[82]

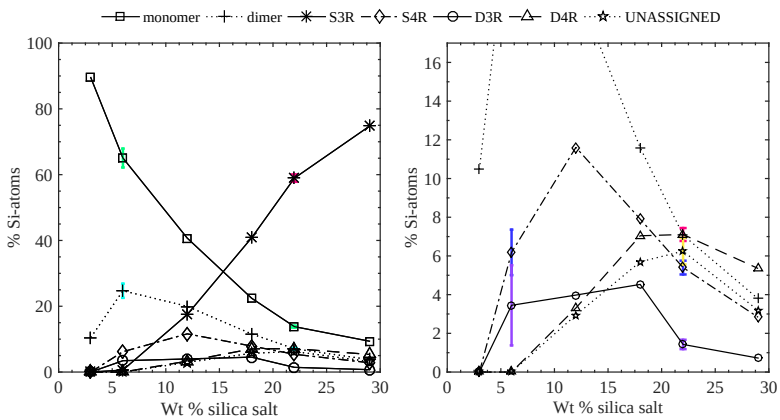


*Figure 4.3: The concentration dependence of the different silica species with increasing silica salt concentration. The error bars for two of the concentrations show the variation between different experiments on equivalent samples. The concentration is given as the number Si atoms in one type of specie in relation to the total number of Si atoms in the solution.*

At the low concentration, 6 wt% silica salt, no cubic octamers are detected by $^{29}$Si-NMR, or at least the signal-to-noise ratio is too low to detect any signal. The solution is instead dominated by the monomers, even though other species are present. The cubic octamer, at this concentrations of Si atoms and $TMA^+$, is hence unstable. An addition of sodium salts (0.1 M or 0.2 M), to this concentration of silica salt, leads to an even larger concentration of the monomer, see figure 4.4. The larger silica species present in the 6 wt% silica salt solutions, hence become more unstable in the presence of sodium atoms. The anionic counterion appears to have less of an effect on the stability of the silica species.

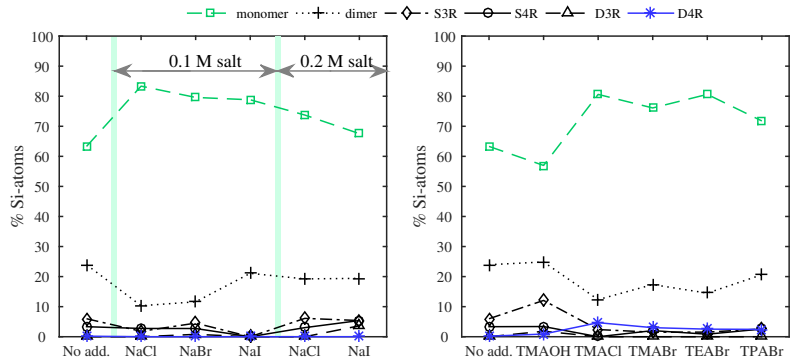


*Figure 4.4: The concentration dependence on the fragmentation, with varying salt additions; 0.1M $TAA^+$ (right) and 0.1 or 0.2 M simple sodium salts (left) to 6wt% silica salt solutions. The D4R are marked with blue stars and the monomer with turquoise squares.*

However, addition of 0.1 M $TAA^+$ ions, to the same Si atom concentration, leads to an increased stability of the cubic octamer, see figure 4.4. At this concentration the length of the alkyl chain is unimportant, all $TAA^+$ ions probed give rise to more or less the same stabilization effect. The anionic counterion appear to have an insignificant impact on the stability of the cubic octamer, as in the case of sodium salt additions. The increase in pH value, originating from the addition of TMAOH, have little effect on the stability of the cubic octamer, but will influence the degree of protonation for the different silica species.

Additions of short chain alcohols, methanol and ethanol, to the previously discussed silica salt solution, have a major effect on the stability of the cube, see figure 4.5. This effect is also apparent in the more concentrated solution (22 wt% silica salt, figure 4.5). Ethanol is, compared to methanol, a more efficient stabiliser and at the higher Si concentration the cubic octamer almost fully retains its structure in its presence. This implies that short chain alcohols enhance stability of larger silica species, or simply protects them from hydrolysis, that may promote fragmentation.

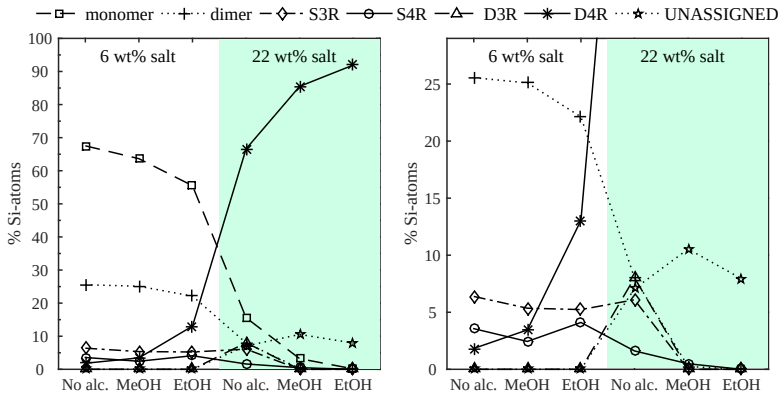


*Figure 4.5: The concentration dependence on the fragmentation with additions of methanol and ethanol to a 6wt% or 22 wt% silica salt solution. The ratio Si to alcohol are kept constant to 1:8.5.*

### 4.1.2 Modelling of the monomer and cubic octamer

The stability of the cube has been attributed to the association of $TMA^+$ to the faces of the cubic octamer, protecting it from hydrolysis.[76,83] The implication was that six $TMA^+$ ions associate, one for each face of the cubic octamer.[83]

A 22 wt% aqueous solution was measured with wide and intermediate angle neutron scattering, and modelled with EPSR. The 22 w% concentration is equivalent to 1 Si: 1 $TMA^+$: 74 $H_2O$. A cubic box, with a side of 71.8 Å, therefore contains 28 monomers, 6 dimers and 14 cubes to 11248 water molecules,with the assumption that only the three most abundant species are important for the solution's behaviour. The concentration of the silicate anion are based on the 29Si-NMR measurements. This model establishes that there is a correlation between both the monomer and cubic octamer to the cationic counterion, $TMA^+$, see figure 4.6. The monomer has a stronger association to the $TMA^+$ compared to that of the cubic octamer. The coordination number, derived from the $Si_{monomer}$-$N_{TMA^+}$ radial distribution function, is approximately 1. The $TMA^+$, being a cation, is expected to associate to the most negative, i.e. the deprotonated, silanol oxygen in the monomer. However the $TMA^+$ has a more preferential association to the protonated oxygens, based on the spatial density function of $Si_{monomer}$-$N_{TMA^+}$. The water, co-

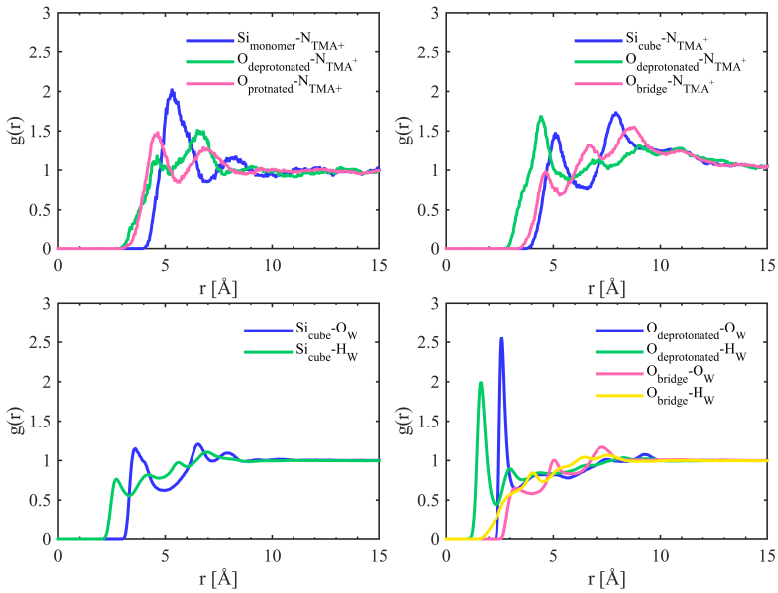


*Figure 4.6: Site-site radial distributions, Si to $N_{TMA^+}$, for the monomer (top left), cubic octamer (top right), and the cubic octamer to water, Si to $O_W$ or $H_W$ (bottom left) and O to $O_W$ or $H_W$ (bottom right).*

ordinate better to the deprotonated silanol oxygen, leaving an available site for polymerisation (even if theTMA$^+$ is highly associated).

The dimer reveals a similar correlation to the TMA$^+$ as for TMA$^+$ to the monomer. The TMA$^+$ preferentially coordinates to the protonated silanol groups, or the siloxane bridge, compared to the deprotonated silanol oxygen.

The association of TMA$^+$ to the cubic octamer appears less strong with a coordination number of only 0.3, for $N_{TMA^+}$ to $Si_{cube}$. This suggest that approximately 3 TMA$^+$ ions associate to the cubic octamer. The $g_{Si_{cube}-N_{TMA^+}}$(r) show the first peak at 5.3 Å and the second at 7.9Å. The TMA$^+$ ions are assumed to be associated to the face of the cube based on he second peak in the $g_{Si_{cube}-N_{TMA^+}}$(r) and the spatial density function, figure 4.7. The spatial density functions shows that the preferred sites of $N_{TMA^+}$ in the first shell around the cube are at the faces. The TMA$^+$

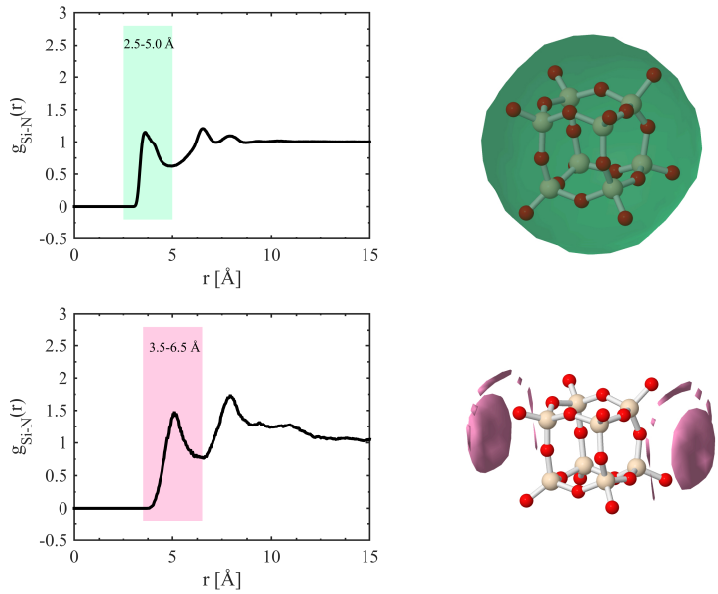


*Figure 4.7: Site-site radial distributions, Si to $O_W$ for the cubic octamer (top left) and the corresponding spatial density function displaying the top 15% probability of finding a $O_W$ around the $Si_{cube}$ between 2.5 - 5.0 Å (top right). The site-site radial distributions, Si to $N_{TMA^+}$ for the cubic octamer (bottom left) and the corresponding spatial density function displaying the top 15% probability of finding a $N_{TMA^+}$ around the $Si_{cube}$ between 3.5 - 6.5 Å (bottom right). These reveal no preferred arrangement of the water around the silicon atoms in the cube, but a higher probability of finding the $N_{TMA^+}$ associated to the faces of the cubic octamer.*

would then occupy positions in an octahedral orientation around the cube. The second closest $TMA^+$, to a Si atom, would then be 7.9 Å apart, which is at the position of the second peak. If the association was different, either at the corners of the edges, the second peak would be at shorter distances to the Si-atom. The water correlation to the different atoms in the cubic octamer, figure 4.6, show that water has no strong preference for either the Si-atoms or the siloxane oxygens, corresponding well to a site being protected by the $TMA^+$ ions. The water does correlate well to the (deprotonated) silanol oxygens, as for the monomers and dimers, leaving the highly negative sites open. Also, both the monomer and the cube exhibit strong anionic character, in the water correlations.

## 4.2 The structure directing agents - SDAs

As previously mentioned the structure directing agents in porous silica materials can be either molecular or supramolecular (molecular for zeolites and supramolecular for mesoporous silica). Their size and ability to interact with silica species in solutions regulates the pore size and affect the structure of the material. Investigation of the SDAs on two levels have been performed. Firstly to establish the their initial state, in aqueous solutions, and, secondly, in the presence of the silica model. The first study is covered in the following two subsections and the second level in the next section.

### 4.2.1 Tetraalkylammonium bromides in aqueous solutions

Tetraallkylammonium ions have both a polar and an apolar part. These opposing characteristics, which as previously mentioned can be altered by changing the length of the alkyl group, will control the aqueous behaviour of these ions. 0.4 M solutions of TMABr and TPABr in water were measured with near and intermediate angle neutron scattering and modelled with EPSR. The behaviour of TMABr and TPABr is remarkably different considering the difference between them is only one methylene group, in each hydrocarbon group.

Based on the water molecules' orientation around the two molecules, it is clear that both display a more hydrophobic than cationic character, see figure 4.8, 4.9 and 4.10. The arrangement in the first shell of

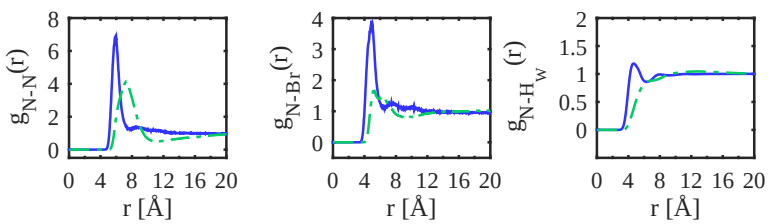


*Figure 4.8: Site-site radial distribution functions for central nitrogen in $TMA^+$ (blue lines) and $TPA^+$ (green dashed lines) to another nitrogen, bromide and hydrogen of water, $H_W$*

the oxygen in the water, $O_W$, around the $TMA^+$, is displayed in figure 4.9 showing the top 15% probability of finding the $O_W$ around the central nitrogen. There is a distinct tetrahedral arrangement of the water

around the $TMA^+$, connecting to both the faces and the edges of the tetrahedron. The equivalent arrangement of water molecules around the $TPA^+$ possesses less of a structure, see figure 4.10. If any structure in the first shell for $TPA^+$ can be claimed, it would be a skew disc inside a sphere. The difference in water arrangement between the two ions is accompanied by a higher degree of hydrophobicity for the $TPA^+$ than the $TMA^+$. $TPA^+$ have a preference to form smaller assemblies of 2-4 ions, while $TMA^+$ ions are free or in pairs. The hydrophobic behavior of

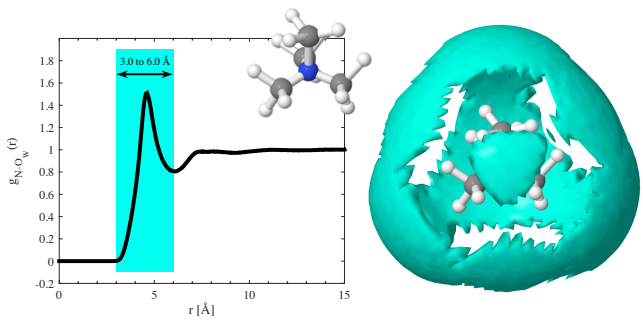


*Figure 4.9: Spatial density functions of the top 15% of the oxygen of water's arrangement around the central nitrogen atom in the $TMA^+$ ion.*

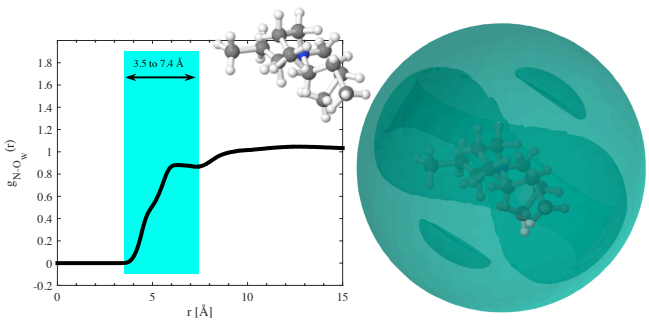


*Figure 4.10: Spatial density functions of the top 15% of the oxygen of water's arrangement around the central nitrogen atom in the $TPA^+$ ion.*

the $TPA^+$ is also manifested in the conformation of the ion, which is far from fully extended. The ions tend to coil up into a spheroid, or oblate; the alkyl chains prefer to interact with each other rather than with water. Even though both ions display a hydrophobic character, they both act as cations. The coordination number, based on the $g_{N_{TAA^+}-Br}$ (figure 4.8), is

approximately 0.5 for both ions, indicating that the bromide ions are not completely dissociated from the $TAA^+$ ions. In contrast to the additives probed in the silica solution, for the $TAA^+$ ions the anionic counterion have different behaviour connected to its identity. Solutions of TMACl have previously been investigated with neutron scattering by Turner *et al*,[28] and reveales an almost complete hydration shell of the chloride ion. A completely hydrated chloride ion is consistent with a more dissociated ion, in contrast to the result for the bromide ion in this study.

### 4.2.2 Decyltrimethylammonium micelles in aqueous solutions

The identity of the anionic counterion in the presence of cationic alkyltrimethylammonium surfactants has, as previously mentioned, a large impact on the micelle properties.[44] The degree of association to the micelle surface is highly dependent on the identity of the counterion, and this will affect the features of the micelles. Due to the expected difference as a consequence of the counterions, five different counterion systems (fluoride, chloride, sulphate, nitrate and p-toluene sulfonate) to the decyltrimethylammonium ($C_{10}TA^+$) surfactant, were measured with near and intermediate angle neutron scattering and conductivity. The neutron scattering data, 0.4 M solutions, was modelled with EPSR, to reconstruct an atomistic description of the micelles and their immediate surrounding, figure 4.11.

EPSR, in the case of micelle systems, locates the largest micelle in the box. Two surfactants are considered to be associated if at least one of the last four carbons in the surfactant tail is closer than 5 Å to another surfactant's four end carbons in the tail. A surface is defined around the largest micelle 1 Å outside the outermost atoms considered to belong to the micelles. The number of nitrogens, from the headgroups, are counted if within 2.5 Å from the inside of the defined surface. This defines the number of positive charges on the micelle surface ($N_{cations}$). The number of counterions associated to the surface ($N_{anions}$) is calculated in a similar manner. If within a distance of 2.5 Å (or 3.0 Å in the $SO_4^{2-}$ system) on either side of the surface, the ions are considered to be associated to the micelle. The degree of dissociation, $\beta$, is defined as $\beta = 1 - {}^{(N_{anions} \cdot z)}/_{N_{cations}}$, where $z$ is the counterion valency. The divalent sulphate ion, has a larger defined distance, due to its preferred location further out from the micelle surface. This has previously been observed in surfactant systems with divalent ions.[43,84,85]

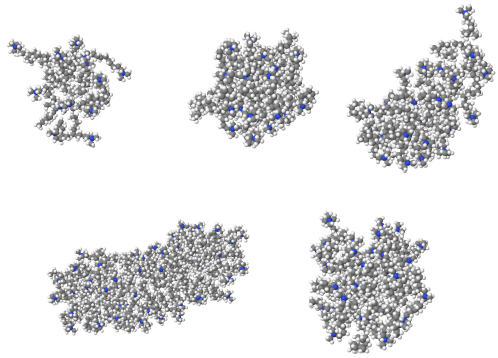

*Figure 4.11: The simulation boxes and largest individual micelle for in the (top left to right) fluoride, chloride, sulphate, (bottom left to right) nitrate and p-toluene sulfonate systems.*

The degree of counterion dissociation, $\beta$, affects a range of the micelle properties. The counterion dissociation was experimentally measured with conductivity, theoretically calculated (from the dressed micelle model devised by Evans *et al.*[53]) and extracted from the EPSR models, see table 4.2. There is an overall trend in the $\beta$-values, for all meth-

*Table 4.2: Counterion dissociation, $\beta$, for the five different systems, from the different techniques.*

| Counterion | $\beta_{conductivity}$ | $\beta^{\dagger}_{dressedmicelle}$ | $\beta_{EPSR}$ |
|---|---|---|---|
| Fluoride | — | 0.93 | $0.92 \pm 0.03$ |
| Chloride | 0.63 | 0.58 | $0.82 \pm 0.02$ |
| Sulpahte | 0.53 | 0.56 | $0.82 \pm 0.04$ |
| Nitrate | 0.32 | 0.32 | $0.66 \pm 0.03$ |
| p-Toluene sulfonate | 0.096 | 0.44 | $0.76 \pm 0.03$ |

$^{\dagger}$The parameters are based on values from the conducttivity measurements (CMC), and simulation (size and aggregation number).

ods. An decrease in counterion dissociation is observed in the order of nitrate, p-toluene sulfonate (p-TS), sulphate, chloride and fluoride, with

exception for the conductivity measurement of the p-TS system. The dissociation obtained from the EPSR models are highly dependent on the distance chosen to define which ions are associated to the surface. This could explain the generally higher values from EPSR compared to those from the dressed micelle model and the conductivity measurements.

A less associated counterion will result in less shielding of the charged headgroups, and as a consequence the surfactants will have a larger effective head group area. A larger headgroup area results in a smaller micelle, due to an increase in the curvature of the self-assembled aggregate. This effect is observed for the five investigated systems; as the counterion dissociation increases the micelles becomes smaller, see table 4.3. The counterion dissociation and size of the micelle, both radius and

*Table 4.3: CMC values, determined via conductivity, radius of gyration ($R_g$), and the averaged aggregation number for the largest micelle in the box for all five systems.*

| Counterion | CMC [mM] | $R_g$ [Å] | Average aggregation number of the largest micelle |
|---|---|---|---|
| Fluoride | 100‡ | 11.1±0.37 | 18 ± 3 |
| Chloride | 90 | 12.6±0.47 | 31 ± 4 |
| Sulpahte | 83 | 13.3±0.34 | 34 ± 2 |
| Nitrate | 60 | 20.4±0.20 | 91 ± 1 |
| p-Toluene sulfonate | 22 | 14.4±1.3 | 47 ± 4 |

‡The CMC value is a linear approximation by Ivanov *et al.*[86]

aggregation number, are in good agreement. The cluster size probabilities can be seen in figure 4.12. The increase in the CMC value in the order fluoride, chloride, sulphate and nitrate correlates well to the decreasing probability of finding smaller clusters in the box. A high cmc is concurrent with a high concentration of free surfactants (or smaller cluster) in solution. The small disagreement between experiments and modeling in the p-TS system is ascribed to the smaller $C_{10}TA^+$ surfactants' ability to elongate in combination with the bulky counterion. The smaller surfactants $C_{10}TA^+$ are not expected to elongate to the same extent as its longer equivalents.[39] As the counterion is fairly large, in comparison to the surface of the micelle, it may impede association.

In the self-assembly process of micelles many forces are at play, and

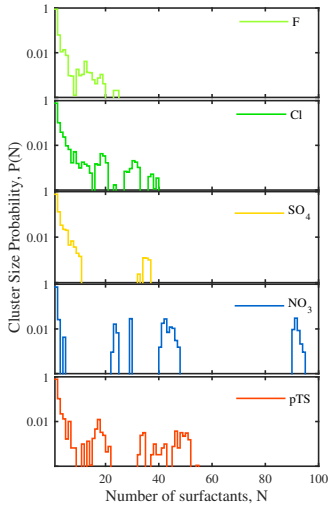


*Figure 4.12: Cluster size probabilities for all five systems.*

it is a delicate balance. The ion-specific effect, often connected to the previously mentioned Hofmeister series, becomes evident after comparing the effect of the ions discussed above. The electrostatic contribution, the action of bringing the charged headgroups close together, is affected by the amount of free ions in solution and the counterion's affinity for the micelle surface. As the background electrolyte increases the length, at which the electrostatic forces work, decreases. Hence, an increase in CMC will lead to a more electrostatically screened system, and the contribution to the overall force will be more affected by the ion-specific effects. Micelle systems is therefore highly influenced by a subtle interplay of these forces.

## 4.3 Structure director agents and silica species in aqueous solutions

The structure directing agent, decyltrimethylammonium bromide, have a stabilising influence on the larger silicate anions, seen by $^{29}$Si-NMR. When 0.4 M $C_{10}$TABr aqueous solutions are mixed with the silica salt, i.e. the cubic octamer, at two different concentrations, 6 wt% and 22 wt%, the cubic octamer is partly able to retain its structure in both solu-

tions. The relative distribution of the Si atoms in the different species can be seen in table 4.4. The two systems were measured with wide and intermediate angle neutron scattering and modelled with EPSR. Due to the low abundance of four of the species in each system, the EPSR models was reduced to only contain two silicate anions each. The two most

*Table 4.4: Relative concentrations of the silicate species, at two different silica salt concentrations (6 wt% and 22 wt%) and in the presence of 0.4 M $C_{10}$TABr, as determined by $^{29}$Si-NMR.*

| Silica addition | monomer | dimer | S3R | S4R | D3R | D4R | unassigned species |
|---|---|---|---|---|---|---|---|
| 6 wt% | 62 % | 24 % | 6.0 % | 2.0 % | 2.4 % | 3.4 % | — |
| 22 wt% | 12 % | 3.8 % | 3.1 % | 2.3 % | 2.6 % | 67 % | 9.2 % |

abundant species in each system was assessed to provide a good representation of each systems. The 6 wt% silica salt sample thus contain only monomers and dimers. The remaining Si atoms was distributed between the monomer and dimer, to preserve the ratio between the two species in the solution. The 22 wt% silica salt model contains monomers and cubic octamers. For this concentrations the smaller silicate ions, containing three or less Si atoms, were considered to be monomers and the Si atoms in the S4R and D3R were considered to be parts of cubic octamers.

The micelles in the EPSR models exhibits a large difference to the $C_{10}$TABr in pure water (Paper II), as the micelles in both systems are much smaller, see table 4.5. The counterion association reveal that almost no anions associate to micelle surfaces in either of the system. A small association of monomer can be found in the low silica concentration model, but no bromide ions are found within the defined distance of 2.5 Å (originates from the distance on either side of the surface that wraps the micelle). A small association of $TMA^+$ ions to the micelle surface is also observed. For the high silica concentration model, equally few anions associate to the micelle surface. Unlike the low concentration model in this model the anion most likely to associate to the micelle surface appear to be the bromide ion, but no silicate anions are found at the surface. This is supported for the site-site radial distribution functions for the Si atoms in the two different models, see figure 4.13 and 4.14. All silicate anions correlate strongly to the $TMA^+$ ion. The $TMA^+$ are

*Table 4.5: Micelle properties from the two EPSR models of SDAs and silicate anions*

| Concentration | 0.4 M $C_{10}$TABr + 6 wt% silica salt | 0.4 M $C_{10}$TABr + 22 wt% silica salt |
|---|---|---|
| Average $N_{agg}$ of the largest micelle | $33 \pm 7$ | $14 \pm 0.33$ |
| Average $R_g$ of the largest micelle | $12.8 \pm 1.3$ | $10.3 \pm 0.15$ |
| Average number of $N_{head}$ at micelle surface | $6 \pm 1$ | $6 \pm 0$ |

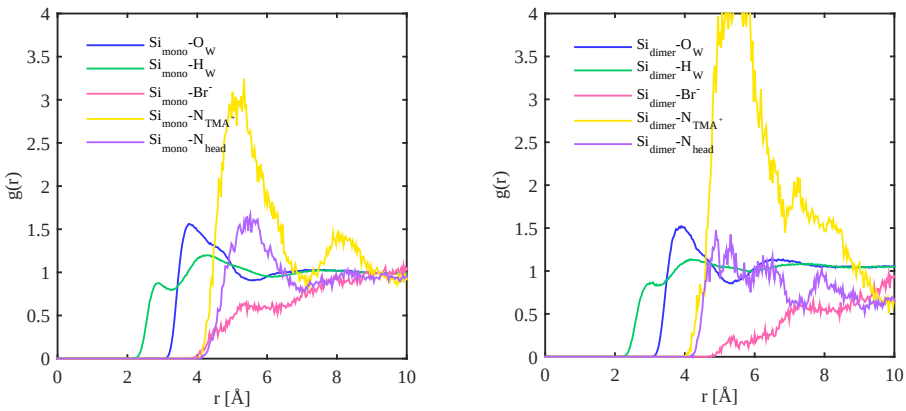


*Figure 4.13: Site-site radial distributions, Si in the monomer to water, bromide, $TMA^+$ and the headgroup (left) and the corresponding distributions for the Si in the dimer (right).*

suggested to be associated to the faces of the cubic octamer, as discussed in the previous section, and will hence not be as free in solutions as the bromide ion. Apparently both the monomer and dimer also prefer associating with the $TMA^+$ instead of the surfactant headgroups.

The decrease in size of the micelle, and difference in counterion association, could partly be explained by electrostatics in combination with ion-specific effect. The bromide are supposed to associate strongly to the micelle surfaces. However, if the predicted degree of ion association for the silicate anions, compared to that of bromide, is lower the increase in free ions might affect the total association of the counterions.

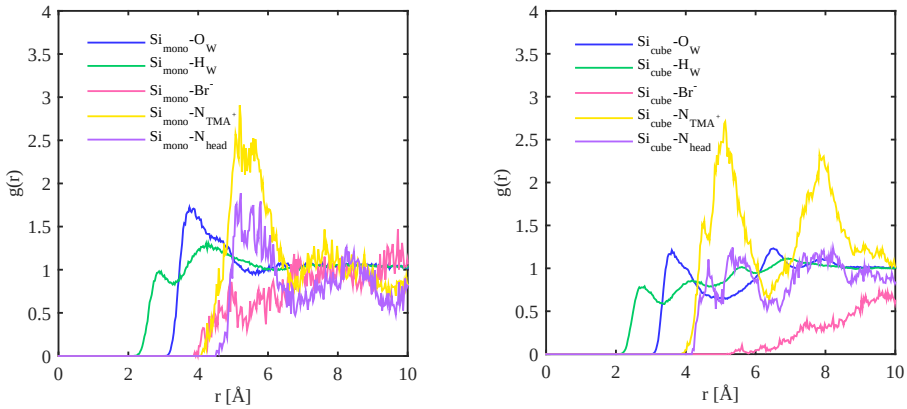


*Figure 4.14: Site-site radial distributions, Si in the monomer to water, bromide, $TMA^+$ and the headgroup (left) and the corresponding distributions for the Si in the cube (right).*

The lack of association of the silicate anions, is in accordance with the observed trend by Frasch *et al.*,[24] who suggested that the silicates species are attracting the surfactants instead of the ions associating to the micelles. However, they observe a higher bromide association than observed in this study.

## 4.4 Conclusions

The aqueous behaviour of $TPA^+$ and $TMA^+$ has been probed using both scattering and EPSR modelling. The $TPA^+$ and $TMA^+$ are both structure directing agents in zeolite syntheses, and the $TMA^+$ is also the inherent counterion to the model silicate anion. Both ions are shown to be hydrophobic, a more dominant behaviour with the larger $TPA^+$. This behaviour is revealed in the clustering of the cations, in both systems, but most apparent in the $TPA^+$ system. The $TPA^+$ ions also adopt a compressed conformation, as if interacting with its own side chains is more beneficial than interacting with water. Even though being hydrophobic, they act as ions, associating to a certain degree to the anionic counterion bromide.

This could explain the different behaviour in the zeolite synthesis; the smaller $TMA^+$ and $TEA^+$ propagate growth while $TPA^+$ and $TBA^+$

initiate nucleation and propagate growth, as shown by Pham *et al.*[87] The larger and more hydrophobic $TAA^+$ ions can stabilise the polymerising, and slightly hydrophobic, silicates and form nuclei for crystal growth. This is supported by the MD simulations by Verstraelen *et al.*[9]who show that the $TPA^+$ stabilise the 10 memberd ring in pure silica ZSM-5 (MFI), and can afterwards be found in the intersections of the channels. The hydrophobic pure silica ZSM-5 (MFI)[6] can allow for more beneficial interactions compared to water, allowing the $TPA^+$ molecule to stretch into an extended conformation.

The cationic surfactants, $C_{10}TA^+$, has been shown to be highly dependent on the counterion present in the aqueous solution. The counterion will affect both size and degree of counterion association. This might affects the size of the pores in the material, but it will definitely influence the range of the electrostatic interactions. The monoatomic counterions, investigated here, follow the expected behaviour in the Hofmeister series. The divalent sulphate reveals that it is a subtle balance between the electrostatic and ion-specific effect which alter the properties of the micelle.

The silicate model, the cubic octamer, fragments into smaller species in aqueous solutions. The fragmentation is highly dependent on additives in the solution. Additives like short chain alcohols and $TAA^+$ ions stabilise the larger species, preferentially the cube, while sodium salts increase the degree of fragmentation into smaller species. The silicate anions, being weak acids, also raise the pH in the system. The fragmentation allows for a differentiation between the silicate anions affinity for the cationic micelles, since there is both smaller and larger species present in the model system.

The silicate anions probed here reveal little affinity for the micelle surface, when the surfactant is $C_{10}TABr$. The presence of silicate anions does, however, highly influence the micelle properties. The micelles decrease substantially compared to the pure water system, and very little anions are found at the surface. The lack of silicates at the micelle surface can stem from a preference of the silica molecules to interact with the smaller and hence mobile $TMA^+$ ions.

# Chapter 5

# Future prospects

Neutron scattering experiments have also been acquired on the $C_{10}TA^+$ systems with different counterions to the surfactant, chloride and sulphate. The fluoride have not been probed together with the silica model as it initiated polymerisation of the silica. The change of counterion will allow us to probe both monoatomic and multi atomic counterions, as well as both divalent and monovalent anions. Hopefully, after the modelling of these systems is complete an elucidation regarding the influence of surfactant counterion on the silica is achieved. Another natural continuation is to increase the complexity in the system, to make it more related to the real MCM-41 synthesis, and add methanol or ethanol to the solution. This influences both the micelles and the silica speciation, the larger species was stabilised. Neutron scattering experiments have been perform on these systems as well, but the modeling is incomplete. This should increase our knowledge concerning the silicas preference for the micelle surface in the pretense of alcohols.

If the different surfactant counterions induce a large difference in the micelle-silica system, synthesis of the MCM-41 material using the different surfactants would be interesting. To which extent would this affect the pore size and the silica network?

A desired system to probe with these techniques would be the surfactant with the cubic octamer as the anionic counterion. This would allow for testing of a system more similar to the actual synthesis. It was shown above that the tetramethylammonium ions have a large affinity for both the silica species and micelles, depending on the concentrations. Hence,

the absence of these would allow for a better probing of the silica species interaction with the structure director.

# Populärvetenskaplig Sammanfattning

Kisel är ett vanligt förekommande grundämne som gärna bildar en oxid, nämligen kiseldioxid. Kiseldioxid träffar man i hög utsträckning på i det dagliga livet. Det är nämligen huvudbeståndsdelen i sand, glasvaror, kvarts, många keramiska material men också i den färgskiftande ädelstenen opal. Det finns också flera grupper av porösa kiseldioxidmaterial, till exempel så kallade zeoliter som har mycket små porer och så kallade mesoporösa material med något större porer. Zeoliter träffar man ofta på i tvättmedel där de fungerar som jonbytare och gör hårt vatten mjukt. Zeoliter används också som katalysatorer och absorptionsmaterial. Mesoporösa material kan användas för bland annat sortering av molekyler, eller som läkemedelsbärare då porstorleken och dess struktur kan påverka tiden för läkemedelsutsöndring.

För att kunna anpassa dessa material efter det ständigt ökande kravet på nya applikationer, hade det varit önskvärt att kunna kartlägga bildandet av dessa ämnen. Hade vi haft total förståelse för hur dessa material bildas så hade vi kunnat, mycket enklare, designa materialen utifrån efterfrågan på deras egenskaper.

Den här studien har syftat på att försöka förstå hur porösa kiseldioxid material byggs upp; hur de olika byggstenarna sätts samman och hur de påverkar varandra. Modelsystem är därför skapat för att likna materialens syntes, men som är förenklade och innehåller bara ett fåtal komponenter. Själva reaktionen går fort och i modellsystemen är det som om vi "stannat tiden" för att få en ögonblicksbild av synteslösningen. Modelleringen, av dessa system, ger oss många ögonblicksbilder vilket ger en översikt av var molekylerna finns i lösning. Med denna förståelse

för molekylerna och deras beteende kan vi förhoppningsvis "styra" dears beteende och bli bättre på att designa materialen.

# References


[1] A. F. Cronstedt, "Observations and descriptions: On an unknown mineral-species called zeolites", in R. v. Ballmoos, J. Higgins, and M. Treacy (eds.), "Proceedings from the Ninth International Zeolite Conference", Butterworth-Heinemann (1993)pp. 3 – 9

[2] M. E. Davis, "Zeolites from a materials chemistry perspective", *Chemistry of Materials* **26** (2014) 239–245

[3] L. M. Ch. Baerlocher and D. Olson (eds.), *Atlas of Zeolite Framework Types*, Elsevier, 6th revised edition edition (2007)

[4] J. Yu, "Chapter 3 synthesis of zeolites", in A. C. Jiří Čejka, Herman van Bekkum and F. Schüth (eds.), "Introduction to Zeolite Science and Practice", volume 168 of *Studies in Surface Science and Catalysis*, Elsevier (2007)pp. 39 – 103

[5] R. M. Barrer and P. J. Denny, "201. hydrothermal chemistry of the silicates. part ix. nitrogenous aluminosilicates", *J. Chem. Soc.* (1961) 971–982

[6] E. M. Flanigen et al., "Silicalite, a new hydrophobic crystalline silica molecular sieve", *Nature* **271** (1978) 512–516

[7] Y. Kubota, M. M. Helmkamp, S. I. Zones, and M. E. Davis, "Properties of organic cations that lead to the structure-direction of high-silica molecular sieves", *Microporous Materials* **6** (1996) 213 – 229

[8] P.-P. E. A. de Moor et al., "Imaging the assembly process of the organic-mediated synthesis of a zeolite", *Chemistry – A European Journal* **5** (1999) 2083–2088

[9] T. Verstraelen et al., "Multi-level modeling of silica-template interactions during initial stages of zeolite synthesis", *Topics in Catalysis* **52** (2009) 1261–1271

[10] C. T. Kresge, M. E. Leonowicz, W. J. Roth, J. C. Vartuli, and J. S. Beck, "Ordered mesoporous molecular sieves synthesized by a liquid-crystal template mechanism", *Nature* **359** (1992) 710–712

[11] Q. S. Huo et al., "Generalized synthesis of periodic surfactant inorganic composite-materials", *Nature* **368** (1994) 317–321

[12] D. Zhao et al., "Triblock copolymer syntheses of mesoporous silica with periodic 50 to 300 angstrom pores", *Science* **279** (1998) 548–552

[13] D. Zhao, Q. Huo, J. Feng, B. F. Chmelka, and G. D. Stucky, "Nonionic triblock and star diblock copolymer and oligomeric surfactant syntheses of highly ordered, hydrothermally stable, mesoporous silica structures", *J. Am. Chem. Soc.* **120** (1998) 6024–6036

[14] J. S. Beck et al., "A new family of mesoporous molecular-sieves prepared with liquid-crystal templates", *J. Am. Chem. Soc.* **114** (1992) 10834–10843

[15] Y. Han et al., "A tri-continuous mesoporous material with a silica pore wall following a hexagonal minimal surface", *Nature Chemistry* **1** (2009) 123–127

[16] R. K. Iler, *The Chemistry of Silica: Solubility, Polymerization, Colloid and Surface Properties and Biochemistry of Silica*, John Wiley and Sons, Inc. (1979)

[17] S. Sjöberg, Y. Hägglund, A. Nordin, and N. Ingri, "Equilibrium and structural studies of silicon(iv) and aluminium(iii) in aqueous solution. v. acidity constants of silicic acid and the ionic product of water in the medium range 0.05–2.0 m na(ci) at 25 °c", *Marine Chemistry* **13** (1983) 35–44

[18] M. T. Anderson, J. E. Martin, J. G. Odinek, and P. P. Newcomer, "Effect of methanol concentration on ctab micellization and on the formation of surfactant-templated silica (sts)", *Chemistry of Materials* **10** (1998) 1490–1500

[19] S. Pevzner and O. Regev, "The in situ phase transitions occurring during bicontinuous cubic phase formation", *Microporous and Mesoporous Materials* **38** (2000) 413–421

[20] S. Q. Liu et al., "The influence of the alcohol concentration on the structural ordering of mesoporous silica: Cosurfactant versus cosolvent", *Journal of Physical Chemistry B* **107** (2003) 10405–10411

[21] I. Beurroies et al., "Detailed in situ xrd and calorimetric study of the formation of silicate/mixed surfactant mesophases under alkaline conditions. influence of surfactant chain length and synthesis temperature", *The Journal of Physical Chemistry B* **110** (2006) 16254–16260, pMID: 16913751

[22] A. Monnier et al., "Cooperative formation of inorganic-organic interfaces in the synthesis of silicate mesostructures", *Science* **261** (1993) 1299–1303

[23] R. Zana et al., "Fluorescence probing investigations of the mechanism of formation of organized mesoporous silica", *Langmuir* **15** (1999) 2603–2606

[24] J. Frasch, B. Lebeau, M. Soulard, J. Patarin, and R. Zana, "In situ investigations on cetyltrimethyl ammonium surfactant/silicate systems, precursors of organized mesoporous mcm-41-type siliceous materials", *Langmuir* **16** (2000) 9049–9057

[25] M. J. Hollamby et al., "Growth of mesoporous silica nanoparticles monitored by time-resolved small-angle neutron scattering", *Langmuir* **28** (2012) 4425–4433, pMID: 22044300

[26] P. Agren et al., "Kinetics of cosurfactant-surfactant-silicate phase behavior. 1. short-chain alcohols", *Journal of Physical Chemistry B* **103** (1999) 5943–5948

[27] A. Firouzi et al., "Alkaline lyotropic silicate,àísurfactant liquid crystals", *Journal of the American Chemical Society* **119** (1997) 3596–3610

[28] J. Turner, A. K. Soper, and J. L. Finney, "A neutron-diffraction study of tetramethylammonium chloride in aqueous-solution", *Molecular Physics* **70** (1990) 679–700

[29] J. Turner, A. K. Soper, and J. L. Finney, "Water-structure in aqueous-solutions of tetramethylammonium chloride", *Molecular Physics* **77** (1992) 411–429

[30] J. Turner and A. K. Soper, "The effect of apolar solutes on water-structure - alcohols and tetraalkylammonium ions", *Journal of Chemical Physics* **101** (1994) 6116–6125

[31] J. Z. Turner, A. K. Soper, and J. L. Finney, "Ionic versus apolar behavior of the tetramethylammonium ion in water", *Journal of Chemical Physics* **102** (1995) 5438–5443

[32] A. K. Soper, J. Turner, and J. L. Finney, "Solute solute correlations in aqueous-solutions of tetramethylammonium chloride", *Molecular Physics* **77** (1992) 431–437

[33] Z. W. Wang and R. G. Larson, "Molecular dynamics simulations of threadlike cetyltrimethylammonium chloride micelles: Effects of sodium chloride and sodium salicylate salts", *Journal of Physical Chemistry B* **113** (2009) 13697–13710

[34] P.-O. Eriksson, G. Lindblom, E. E. Burnell, and G. J. T. Tiddy, "Influence of organic solutes on the self-diffusion of water as studied by nuclear magnetic resonance spectroscopy", *Journal of the Chemical Society, Faraday Transactions 1: Physical Chemistry in Condensed Phases* **84** (1988) 3129–3139

[35] D. Bhowmik et al., "Aqueous solutions of tetraalkylammonium halides: ion hydration, dynamics and ion-ion interactions in light of steric effects", *Physical Chemistry Chemical Physics* **16** (2014) 13447–13457

[36] J. T. Slusher and P. T. Cummings, "Molecular simulation study of tetraalkylammonium halides .1. solvation structure and hydrogen bonding in aqueous solutions", *Journal of Physical Chemistry B* **101** (1997) 3818–3826

[37] H. Krienke, V. Vlachy, G. Ahn-Ercan, and I. Bako, "Modeling tetraalkylammonium halide salts in water: How hydrophobic and electrostatic interactions shape the thermodynamic properties", *Journal of Physical Chemistry B* **113** (2009) 4360–4371

[38] N. Huang et al., "Microscopic probing of the size dependence in hydrophobic solvation", *The Journal of Chemical Physics* **136** (2012) 074507

[39] K. Holmberg, B. Jönsson, B. Kronberg, and B. Lindman, *Surfactants and polymers in aqueous solution*, John Wiley and Sons, Ltd, 2 edition (2003)

[40] D. F. Evans and H. Wennerström, *The Colloidal Domain: Where Physics, Chemistry, Biology, and Technology Meet*, Wiley-VHC, New York, 2nd edition (1999)

[41] D. Varade, K. Aramaki, and C. Stubenrauch, "Phase diagrams of water-alkyltrimethylammonium bromide systems", *Colloids and Surfaces a-Physicochemical and Engineering Aspects* **315** (2008) 205–209

[42] G. Gunnarsson, B. Jonsson, and H. Wennerstrom, "Surfactant association into micelles - an electrostatic approach", *Journal of Physical Chemistry* **84** (1980) 3114–3121

[43] H. Wennerstrom, A. Khan, and B. Lindman, "Ionic surfactants with divalent counterions", *Advances in Colloid and Interface Science* **34** (1991) 433–449

[44] N. Jiang et al., "Aggregation behavior of hexadecyltrimethylammonium surfactants with various counterions in aqueous solution", *Journal of Colloid and Interface Science* **286** (2005) 755–760

[45] C. Gamboa, H. Rios, and L. Sepulveda, "Effect of the nature of counterions on the sphere-to-rod transition in cetyltrimethylammonium micelles", *The Journal of Physical Chemistry* **93** (1989) 5540–5543

[46] D. F. Parsons, M. Bostrom, P. Lo Nostro, and B. W. Ninham, "Hofmeister effects: interplay of hydration, nonelectrostatic potentials, and ion size", *Physical Chemistry Chemical Physics* **13** (2011) 12352–12367

[47] P. Jungwirth and P. S. Cremer, "Beyond hofmeister", *Nature Chemistry* **6** (2014) 261–263

[48] M. Bostrom, D. R. M. Williams, and B. W. Ninham, "Ion specificity of micelles explained by ionic dispersion forces", *Langmuir* **18** (2002) 6010–6014

[49] M. Lund, R. Vacha, and P. Jungwirth, "Specific ion binding to macromolecules: Effects of hydrophobicity and ion pairing", *Langmuir* **24** (2008) 3387–3391

[50] T.-M. Perger and M. Bešter-Rogač, "Thermodynamics of micelle formation of alkyltrimethylammonium chlorides from high performance electric conductivity measurements", *Journal of Colloid and Interface Science* **313** (2007) 288–295

[51] G. M. Roger et al., "Interpretation of conductivity results from 5 to 45 °c on three micellar systems below and above the cmc", *The Journal of Physical Chemistry B* **112** (2008) 16529–16538

[52] R. Zana, S. Yiv, C. Strazielle, and P. Lianos, "Effect of alcohol on the properties of micellar systems", *Journal of Colloid and Interface Science* **80** (1981) 208 – 223

[53] D. F. Evans, D. J. Mitchell, and B. W. Ninham, "Ion binding and dressed micelles", *Journal of Physical Chemistry* **88** (1984) 6344–6348

[54] J. B. Hayter, "A self-consistent theory of dressed micelles", *Langmuir* **8** (1992) 2873–2876

[55] I. Chakraborty, , and S. P. Moulik*, "Self-aggregation of ionic c10 surfactants having different headgroups with special reference to the behavior of decyltrimethylammonium bromide in different salt environments:,Äâ a calorimetric study with energetic analysis", *The Journal of Physical Chemistry B* **111** (2007) 3658–3664, pMID: 17388531

[56] D. H. Williams and I. Fleming, *Spectroscopic Methods in Organic Chemistry*, McGraw-Hill publishing company, fifth edition (1995)

[57] P. J. Hore, *Nuclear Magnetic Resonance*, Oxford University Press Inc. (1995)

[58] P. Lindner and T. Zemb (eds.), *Neutron, X-rays and Light: Scattering Methods Aplied to Condensed Matter*, North-Holland Delta Series, second edition (2002)

[59] A. K. Soper, *GudrunN and GudrunX: programs for correcting raw neutron and X-ray diffraction data to differential scattering cross section* (2011)

[60] J. E. Enderby, "Ion solvation via neutron-scattering", *Chemical Society Reviews* **24** (1995) 159–168

[61] V. F. Sears, "Neutron scattering lengths and cross sections", *Neutron News* **3** (1992) 26–37

[62] J. L. Finney and A. K. Soper, "Solvent structure and perturbations in solutions of chemical and biological importance", *Chemical Society Reviews* **23** (1994) 1–10

[63] A. K. Soper, "Empirical potential monte carlo simulation of fluid structure", *Chemical Physics* **202** (1996) 295–306

[64] A. K. Soper, "Tests of the empirical potential structure refinement method and a new method of application to neutron diffraction data on water", *Molecular Physics* **99** (2001) 1503–1516

[65] A. K. Soper, "Partial structure factors from disordered materials diffraction data: An approach using empirical potential structure refinement", *Physical Review B* **72** (2005) 12

[66] A. K. Soper, "Joint structure refinement of x-ray and neutron diffraction data on disordered materials: application to liquid water", *Journal of Physics: Condensed Matter* **19** (2007) 335206

[67] R. L. McGreevy, "Reverse monte carlo modelling", *Journal of Physics: Condensed Matter* **13** (2001) R877

[68] A. K. Soper, *Empirical Potential Structure Refinement - EPSRshell. A User's Guide*, version 24 edition (2015)

[69] P. Murkerjee and K. J. Mysels, *Critical Micelles Concentrations in Aqueous Surfactant Ssytems*, volume 36, National Standard Reference Data Systems, National Bureau of Standards (1971)

[70] R. Zana, "Ionization of cationic micelles: Effect of the detergent structure", *Journal of Colloid and Interface Science* **78** (1980) 330–337

[71] R. K. Harris and C. T. G. Knight, "Silicon-29 nmr studies of aqueous silicate solutions: Part iv. tetraalkylammonium hydroxide solutions", *Journal of Molecular Structure* **78** (1982) 273–278

[72] S. D. Kinrade and T. W. Swaddle, "Silicon-29 nmr studies of aqueous silicate solutions. 1. chemical shifts and equilibria", *Inorganic Chemistry* **27** (1988) 4253–4259

[73] R. K. Harris and C. T. G. Knight, "Si-29 nuclear magnetic-resonance studies of aqueous silicate solutions .5. 1st-order patterns in potassium silicate solutions enriched with si-29", *Journal of the Chemical Society-Faraday Transactions Ii* **79** (1983) 1525–1538

[74] C. J. Brinker and G. W. Scherer, *Sol-Gel science: the physics and chemistry of sol-gel processing*, Academic press, San Diego (1990)

[75] W. M. Hendricks, A. T. Bell, and C. J. Radke, "Effects of organic and alkali-metal cations on the distribution of silicate anions in aqueous-solutions", *Journal of Physical Chemistry* **95** (1991) 9513–9518

[76] S. D. Kinrade, C. T. G. Knight, D. L. Pole, and R. T. Syvitski, "Silicon-29 nmr studies of tetraalkylammonium silicate solutions. 1. equilibria, si-29 chemical shifts, and si-29 relaxation", *Inorganic Chemistry* **37** (1998) 4272–4277

[77] S. D. Kinrade, C. T. G. Knight, D. L. Pole, and R. T. Syvitski, "Silicon-29 nmr studies of tetraalkylammonium silicate solutions. 2. polymerization kinetics", *Inorganic Chemistry* **37** (1998) 4278–4283

[78] M. Haouas and F. Taulelle, "Revisiting the identification of structural units in aqueous silicate solutions by two-dimensional silicon-29 inadequate", *Journal of Physical Chemistry B* **110** (2006) 3007–3014

[79] C. T. G. Knight, R. J. Balec, and S. D. Kinrade, "The structure of silicate anions in aqueous alkaline solutions", *Angewandte Chemie-International Edition* **46** (2007) 8148–8152

[80] M. Haouas, D. P. Petry, M. W. Anderson, and F. Taulelle, "Si-29 nmr relaxation of silicated nanoparticles in tetraethoxysilane-tetrapropylammonium hydroxide-water system (teos-tpaoh-h2o)", *Journal of Physical Chemistry C* **113** (2009) 10838–10841

[81] D. P. Petry et al., "Connectivity analysis of the clear sol precursor of silicalite: Are nanoparticles aggregated oligomers or silica particles?", *Journal of Physical Chemistry C* **113** (2009) 20827–20836

[82] I. Hasegawa, S. Sakka, K. Kuroda, and C. Kato, "The effect of tetramethylammonium ions on the distribution of silicate species in the methanolic solutions", *Journal of Molecular Liquids* **34** (1987) 307–315

[83] S. Caratzoulas, D. G. Vlachos, and M. Tsapatsis, "Molecular dynamics studies on the role of tetramethylammonium cations in the stability of the silica octamers si8o208- in solution", *Journal of Physical Chemistry B* **109** (2005) 10429–10434

[84] A. Khan, K. Fontell, and B. Lindman, "Liquid crystallinity in systems of magnesium and calcium surfactants: Phase diagrams and phase structures in binary aqueous systems of magnesium and calcium di-2-ethylhexylsulfosuccinate", *Journal of Colloid and Interface Science* **101** (1984) 193–200

[85] D. Maciejewska, A. Khan, and B. Lindman, "Hexadecyltrimethyl ammonium sulphate-water system. phase diagram and micellization", *Progress in Colloid  Polymer Science* **73** (1987) 174–179

[86] I. B. Ivanov, R. I. Slavchov, E. S. Basheva, D. Sidzhakova, and S. I. Karakashev, "Hofmeister effect on micellization, thin films and emulsion stability", *Advances in Colloid and Interface Science* **168** (2011) 93–104

[87] T. C. T. Pham, H. S. Kim, and K. B. Yoon, "Growth of uniformly oriented silica mfi and bea zeolite films on substrates", *Science (New York, N.Y.)* **334** (2011) 1533–8

# Acknowledgements

There are several persons who have participated in making this thesis reality, and who I would especially like to acknowledge.

I would like to start by thanking my supervisor, Viveka Alfredsson, for encouraging me to do a PhD. You have constantly supported and encouraged me; when the project has not developed the way we wanted (or at all...) or the few times something actually did work. It has motivated me to master things I never thought possible. I'm forever grateful that you have showed me the world of science, and how rewarding and fun it can be.

I would also like to thank my co-supervisors, Olle Söderman och Sven Lidin. You have helped me when I need it, and you have always taken the time to discuss with me and answer all my questions.

Another recognition goes to Karen Edler, even though technically not my supervisor, you have treated me as one of your own students. You introduced me to the "wonderful" world of neutron scattering and I'll always be grateful for that. Thank You.

Our collaborator Daniel Bowron for *all* the indispensable help with the EPSR program!

No to mention Majlis Larsson, Ingrid Nilsson och Helena Persson, for taking care of all the administrative work, Maria Södergren for all the practical assistance and Christopher Hirst for all technical (and other) support over the years. Thank you, without all of you nothing would ever happen at the division!

A huge *thank you* goes all members at the Division of Physical Chemistry, past and present. Without all of you this would never have happened. I will miss all the discussions, scientific or otherwise, the punctual coffee breaks but mostly all the laughters and amazing persons.

I would also especially like to thank Saskia, Solmaz, Johanna, Divya and Jessie! You have all participated in making these years such a pleasant experience. For all the memories we have together; weddings, travels, celebrations, discussions, dinners, linners, lunches, laughters and tears. I hope theee will be many more to come, because I am so grateful for our friendship.

Maria, Filip, Sofia och Annika, tack för alla luncher genom åren, för alla skratt och (o)vetenskapliga diskussioner. De har många gånger varit en önskvärd paus som fått en att orka lite till.

Ett stort tack går till alla mina vänner, speciellt Emma, Helena, Jasmine och Jessica, för att ni på så många sätt agerat som motpol till min vardag, men framförallt för att ni alltid funnits där för mig!

Till sist vill jag tacka min familj, Marie, Gert och Björn (och även du Rikard), för att ni alltid ovillkorligen ställer upp för mig, och för det otroliga stöd jag vet att jag alltid har från er! Jag hoppas att ni vet hur tacksam jag är för er alla, för det går inte att beskriva med ord.

Printed by Media-Tryck, Lund University


ISBN 978-91-7422-452-8

Physical Chemistry
Faculty of Science
Lund University